REPORT DOCUMENTATION PAGE

Form Approved
OMB No. 0704-0188

1. AGENCY USE ONLY (Leave blank)	2. REPORT DATE	3. REPORT TYPE AND DATES COVERED
	31.12.96	Final - Oct 1995-Dec 1996

4. TITLE AND SUBTITLE
Final Report on Phase 2 using Geostatistics for Data Comprehension and Reconstruction of Remote Imagery

5. FUNDING NUMBERS
PR-N68171
95-C-128

6. AUTHOR(S)
Dr M A Oliver, Professor R Webster

7. PERFORMING ORGANIZATION NAME(S) AND ADDRESS(ES)
University of Reading, Whiteknights,
Reading, RG6 2AH, UK

8. PERFORMING ORGANIZATION REPORT NUMBER
RSS USA-2/4

9. SPONSORING/MONITORING AGENCY NAME(S) AND ADDRESS(ES)
USARDSG-UK, Environmental Sciences Branch
Edison House, 233 Old Marylebone Road,
London, NW1 5TH, UK

10. SPONSORING/MONITORING AGENCY REPORT NUMBER

11. SUPPLEMENTARY NOTES
Final Report

12a. DISTRIBUTION/AVAILABILITY STATEMENT
No limitation on distribution/availability

12b. DISTRIBUTION CODE

13. ABSTRACT (Maximum 200 words)

This report contains a summary of two of the three earlier interim reports together with the most recent results on image restoration. In addition to the analysis of the remotely sensed data we investigated Paul Krauser's climatic data (Part I). The climatic variables for the eastern USA were estimated by both auto- and co-kriging, and the results compared with the validation data. In general co-kriging produced more precise estimates than auto kriging. Part II contains a brief evaluation of Genstat and Isatis for geostatistical analysis. Part III describes the results of an optimal sampling analysis, of kriging from the SPOT information at Fort Benning and of a kriging analysis to filter the imagery so that the short- and long-range structures present could be distinguished more clearly. Part IV describes the most recent work on data compression and reconstruction. Part of the original area was chosen for this analysis and then sampled at different intensities. The sample data were used for estimation with the variogram model by kriging and conditional Gaussian sequential simulation. The results show that with a good variogram model it is possible to restore the data well from 25% of the original values. Kriging provides the more precise local values, but simulation retains the original degree of variation.

14. SUBJECT TERMS	15. NUMBER OF PAGES
Co-kriging, cross variograms, filtering, geostatistics, image restoration, kriging, optimal sampling, spatial scale, variogram	16. PRICE CODE

17. SECURITY CLASSIFICATION OF REPORT	18. SECURITY CLASSIFICATION OF THIS PAGE	19. SECURITY CLASSIFICATION OF ABSTRACT	20. LIMITATION OF ABSTRACT

TABLE OF CONTENTS

LIST OF TABLES

TABLE OF FIGURES

PREFACE

This report was sponsored by the United States Army Research, Development and Standardization Group-UK (USARDGSG-UK), London, NW1 5TH, United Kingdom, under contract PR-N 68171-95-C-9128, entitled, "Using Geostatistics for Data Compression and Reconstruction of Remote Imagery - Phase 2", and is monitored by the U. S. Army Topographic Engineering Center (TEC), Alexandria, Virginia 22315-3863. The work was done by the University of Reading, Whiteknights, Reading, RG6 6DW, United Kingdom. The USARDGSG-UK Program Manager is Mr. Jerry Comati, and the TEC Contracting Officer's Representative is Mr. Kevin Slocum.

EXECUTIVE SUMMARY

This report contains a summary of two of the three earlier interim reports together with the most recent results on image reconstruction. At the outset of this phase of the project the intention was to work at Fort Belvoir so that ground information could be obtained more readily. The first report that we did for this project described the site and the proposals. After Dr Oliver's visit to TEC in February 1996 Mr Slocum and his team decided that we could achieve more in the time by continuing to work on the Fort Benning data. This would avoid the preliminary data analysis of Fort Belvoir that had already been done for Fort Benning. There was still much to do on the Fort Benning data, as will be seen from Parts III and IV of this report. In addition to the work on the remotely sensed data we were also asked to investigate Paul Krause's climate data (Part I) and to evaluate Genstat and Isatis for geostatistical analysis (Part II). Part of the analysis of the climate data was carried out while Dr Oliver was at TEC in February 1996; the remainder was done in the U. K. The climatic variables for the eastern U. S. A. were estimated by both auto- and cokriging, and the results compared with the validation data. In general cokriging produced more precise estimates than autokriging. Part III describes the results of an optimal sampling analysis, of kriging from the SPOT information at Fort Benning and of a kriging analysis to filter the imagery so that the short- and long-range structures present could be distinguished more clearly. The final section of the report (Part IV) describes the most recent work on data compression and reconstruction. Part of the original area analysed was chosen for this analysis. The 10 000 pixels of Benncut were sampled at different intensities. The sample data were then used for estimation with the variogram model by kriging and conditional Gaussian sequential simulation. We compare the results of these two methods for reconstructing the image information after removing a large proportion of the data. The results show that with a good variogram model it is possible to restore the data well from 25% of the original values. Kriging provides the more precise local values, but simulation retains the original degree of variation.

PART I: A COMPARISON OF GENSTAT AND ISATIS

For this part of the project we were asked to compare Isatis with Genstat. Isatis is a package designed specifically for geostatistics, whereas Genstat is much more general, though it now contains routines for geostatistics. In the event we did not have Isatis, and so we could not evaluate it adequately or compare it fairly with Genstat (Genstat 5 Committee, 1987. We treat Isatis very briefly therefore before describing Genstat in more detail.

Isatis is the third of a series of geostatistical programs written by staff of the Centre de Géostatistique of the Paris School of Mines. In these the basic algorithms have remained much the same, but the interface to the user has been much improved in the light of experience. The program contains a comprehensive set of routines for geostatistical analysis that can be used readily from a menu. This enables the user to progress rapidly in the initial stages of an investigation. It has no programming language, and so if users want facilities that are not in the menu then they must leave the program and resort to other tools. Thus, lack of flexibility might prove a disadvantage, especially when the user has gained expertise in the subject.

Genstat has similarly evolved over time. In its early versions operations were specified by commands. These could be embodied in programs using the Genstat language, and this programming environment is still available. The new version of the program for Windows provides a menu as an alternative, and so users can choose which mode they prefer, and they can switch from to the other. Genstat is very general and powerful. It provides facilities for most of the standard statistical analyses, tabulation and high quality graphics, and the latest release includes advanced techniques based on recent research in statistical computing. It has a large multivariate library. Because it can be programmed it is completely flexible, and there is no need to leave the Genstat environment as demand changes. For geostatistics it is important because it has the facility for fitting several non-linear variogram models. This is the most difficult part of geostatistics in general and also the one for which most software is deficient.

Geostatistics in Genstat

Genstat now embodies a suite of techniques for analysing data distributed in a space of one or two dimensions geostatistically. It includes commands for computing experimental variograms and for estimating (predicting) by ordinary kriging, and it has a special procedure for fitting the common non-linear models to experimental variograms.

Starting with a set of data the three operations proceed in sequence, as follows.

(1) Estimate semivariances at discrete lags to form an ordered set; the sample or

experimental variogram.

(2) Fit plausible models from those allowed to the experimental variogram.

(3) Krige.

These are called by three directives, which are described in Appendix 1. In many applications the purpose of kriging is to make a map. Values are then kriged at the nodes of a fine grid, through which isarithms, 'contours', can then be threaded. Kriging is implemented in Genstat with this in view.

Since this report was compiled it was suggested that the version of Genstat for workstations should be used because of the need to analyse large data sets of remotely sensed data. This version works with the command language. The directives for geostatistics remain the same (see Appendix 1).

PART II: KRIGING AND COKRIGING OF CLIMATE DATA

Data and method

Paul Krause (TEC) provided us with data from 177 weather recording stations in the eastern USA for geostatistical analysis. The full set of data was divided into two subsets; one consisting of 121 sites, the other of 56 sites that constituted a validation set at which estimates from the first could be compared with recorded values. The variables in the data were height, potential evaporation, continentality, mrange and temperature. We computed auto and cross variograms for these properties. The auto variograms were then modelled using Ross's MLP (Maximum Likelihood Program) (Ross, 1987). This was while Margaret Oliver was at TEC in February 1996. Using these variograms and both the full and test sets of data the values of each property were estimated by ordinary autokriging at more than 5000 sites. Both sets of estimates for temperature were then used for mapping. The autokriged estimates for the test data matched those of the full set well.

Table 1 summarizes the data. Among other things it shows that height was strongly skewed, and that taking square roots of height made the distribution more nearly symmetric and would thereby stabilize variances in later analyses. The correlations between the variables (Table 2) were weak to moderate. Of particlar interest were the correlations between height and the climatic variables (column 2, Table 2). That for height and mrange was the strongest, whereas that between height and temperature was the weakest.

The coregionalizations of height and of the other variables separately were analysed by computing experimental auto and cross variograms and then modelling them (Wackernagel, 1994). The cross variance between two random variables u and v obeying the Intrinsic Hypothesis is defined by

$$\gamma_{uv}(\mathbf{h}) = \frac{1}{2}\mathrm{E}[\{Z_u(\mathbf{x}) - Z_u(\mathbf{x}+\mathbf{h})\}\{Z_v(\mathbf{x}) - Z_v(\mathbf{x}+\mathbf{h})\}] , \qquad (1)$$

where $Z_u(\mathbf{x})$, $Z_v(\mathbf{x})$, $Z_u(\mathbf{x}+\mathbf{h})$, and $Z_v(\mathbf{x}+\mathbf{h})$ are the values of the two variables at any two places $\mathbf{x}$ and $\mathbf{x}+\mathbf{h}$ separated by the vector $\mathbf{h}$. As a function of $\mathbf{h}$ $\gamma_{uv}(\mathbf{h})$ is the cross variogram. Values of $\gamma_{uv}(\mathbf{h})$ can be estimated from data by calculating experimental or sample cross variances using the usual computing formula:

$$\hat{\gamma}_{uv}(\mathbf{h}) = \frac{1}{2m(\mathbf{h})}\sum_{i=1}^{n}\{z_u(\mathbf{x}_i) - z_u(\mathbf{x}_i+\mathbf{h})\}\{z_v(\mathbf{x}_i) - z_v(\mathbf{x}_i+\mathbf{h})\} , \qquad (2)$$

where now $z_u(\mathbf{x}_i)$, $z_v(\mathbf{x}_i)$, $z_u(\mathbf{x}_i+\mathbf{h})$, and $z_v(\mathbf{x}_i+\mathbf{h})$ are measured values of the two variables at sampling points $\mathbf{x}_i$ and $\mathbf{x}_i+\mathbf{h}$, of which there are m pairs separated by $\mathbf{h}$. Changing $\mathbf{h}$ gives an ordered set of cross variances, the experimental cross variogram.

Table 1: Summary statistics for climatic data.

	Height	Square root height	Potential evapo-transpiration	Contin-entality	Mrange	Temp-erature
Minimum	3	1.7	19.2	9.3	42	23.0
Maximum	3945	62.8	197.3	59.3	106	76.7
Mean	676	22.0	82.9	40.1	84.7	48.9
Median	500	22.3	83.8	41.1	86	46.2
St. deviation	767	13.9	31.2	9.19	11.0	13.3
Variance	588 450	194.4	973.5	84.34	120.5	178.5
Skew	2.0	0.57	0.84	−0.70	−0.91	0.28

To complete the coregionalization the variograms for all combinations of u and v are computed. When $u = v$ one obtains the usual auto variogram. So the coregionalization for two variables, as here, involves computing two autovariograms, one for each of u and v, and one cross variogram.

Modelling the coregionalization involves fitting an authorized model to the whole set of experimental variograms. As for a single variable, the model must be such as to ensure that any weighted combination of values of the variables has a non-negative variance. The same set of authorized functions is available to choose from. There is an additional constraint, however, explained below.

We suppose that the three variograms, the two auto variograms and the cross variogram, are linear combinations of K basic variogram functions, $g^k(\mathbf{h}), k = 1, 2, \ldots, K$:

$$\gamma_{uv}(\mathbf{h}) = \sum_{k=1}^{K} b_{uv}^k g^k(\mathbf{h}) , \tag{3}$$

where b_{uv}^k is the coefficient of the basic variogram $g^k(\mathbf{h})$ in the model. This is the linear model of coregionalization. In the bivariate case, which is all we are concerned with here, the linear model is valid if the $g^k(\mathbf{h})$ are all legitimate functions for variograms and the coefficients b_{uv}^k satisfy the conditions:

$$b_{uu}^k \geq 0, \qquad b_{vv}^k \geq 0 ,$$

Table 2: Correlation matrix in lower triangle.

Square root height	1				
Potential evapotranspiration	–0.354	1			
Continentality	0.607	–0.158	1		
Mrange	0.703	–0.248	0.770	1	
Temperature	–0.440	–0.272	–0.776	–0.495	1

and

$$|b^k_{uv}| \;=\; |b^k_{uv}| \leq \sqrt{b^k_{uu} b^k_{vv}}\ .$$

This latter condition is Schwarz's inequality.

Goulard & Voltz (1992) devised an algorithm for fitting linear models with these constraints, and it the one we used for this research. After inspecting the forms of the variograms and judging the distance parameters we fitted the most plausible models and thereby obtained values for the linear parameters. In the event we found that in all cases we could model the experimental variograms by combinations of nugget plus isotropic power functions. The general equation is

$$\gamma(h) \;=\; b_1 + b_2 h^{\alpha}\ , \tag{4}$$

where b_1 is the nugget variance, b_2 is the coefficient of the power term, and α is the exponent, which varied from case to case. Table 3 lists the parameters and their values.

Having obtained a valid model for the coregionalization we proceded to cokrige. Cokriging is the logical extension of univariate or autokriging to situations where two or more variables are spatially interdependent. As in autokriging, page 11, the aim is to estimate values of a variable, $Z(\mathbf{x})$, at a set of points or in one or more blocks, which we shall denote by $\mathbf{x}_0$ for generality, from data on Z *plus* the related data on the other variable(s).

Using the same notation as above we suppose that we wish to predict values of variable u, or in full $Z_u(\mathbf{x})$, and we suppose that this variable is less densely sampled than the other, v. In ordinary cokriging we form the linear sum

$$\widehat{Z}_u(\mathbf{x}_0) \;=\; \sum_{l=1}^{2} \sum_{i=1}^{n_l} \lambda_{il} z_l(\mathbf{x}_i)\ , \tag{5}$$

where the subscript l refers to the variables, and the subscript i refers to the sites, of which there are n_l where the variable l has been measured. We want the estimate to be unbiased, and so the weights λ_{il} sum as follows:

$$\sum_{i=1}^{n_l} \lambda_{il} = 1, \quad l = u; \quad \text{and} \quad \sum_{i=1}^{n_l} \lambda_{il} = 0, \quad l \neq u \ .$$

In words, the weights for the target variable u sum to 1, and those for v sum to zero. Then for $v = 1, 2$ and for all $j = 1$ to n_v we form the equations

$$\sum_{l=1}^{2} \sum_{i=1}^{n_l} \lambda_{il} \gamma_{lv}(\mathbf{x}_i, \mathbf{x}_j) + \psi_v \quad = \quad \gamma_{uv}(\mathbf{x}_j, \mathbf{x}_0) \ . \tag{6}$$

The quantity $\gamma_{lv}(\mathbf{x}_i, \mathbf{x}_j)$ is the cross semivariance between variables l and v at sites i and j, separated by the vector $\mathbf{x}_i - \mathbf{x}_j$, $\gamma_{uv}(\mathbf{x}_j, \mathbf{x}_0)$ is the average (cross) semivariance between a site j and the point $\mathbf{x}_0$, and ψ_v is the Lagrange multiplier for the vth variable. The full cokriging system is thus

$$\begin{aligned} \sum_{l=1}^{2} \sum_{i=1}^{n_l} \lambda_{il} \gamma_{lv}(\mathbf{x}_i, \mathbf{x}_j) + \psi_v \quad &= \quad \gamma_{uv}(\mathbf{x}_j, \mathbf{x}_0) \ \ \forall\, v = 1, 2 \ \ \forall\, j = 1, 2, \ldots, n_v \\ \sum_{i=1}^{n_u} \lambda_{iu} \quad &= \quad 0 \\ \sum_{j=1}^{n_l} \lambda_{jl} \quad &= \quad 0 \ \ \forall\, l \neq u \ . \end{aligned} \tag{7}$$

It is solved to obtain the weights, which are inserted into Equation (5) to estimate $Z_u(\mathbf{x}_0)$.

Using the models of Table 3 and the coordinates in the data we set up the kriging systems above for punctual cokriging with the square root of topographic height as the subsidiary variable, v above, and the other four variables, potential evaporation, continentality, mrange and temperature, as the target variables, u, in turn. In each case we predicted u at the 56 validation sites in three ways. These were:

(1) autokriging from the 121 sites of the first set of data;
(2) cokriging from the 121 sites;
(3) cokriging from the test variable and height at the 121 sites plus height at the 56 validation sites.
4) In addition, because we knew the height at all the sites of the validation set, we could use simple regression to predict the target variables, and we did this also.

For each method and for each point we computed the error as the difference between the estimate and the recorded value, the squared error and the kriging variance. We

then computed their averages and the ratio of the mean squared error to the kriging variance.

Results

The individual estimates at the 56 validation sites and their variances are given in Tables 1 to 4 in Appendix 2 together with the measured values there. The summaries of these results are tabulated in Table 4.

Table 4 shows that the bias, as represented by the mean error, is negligible. The kriging variance diminishes consistently as more information is included, as it should. Autokriging incurs the largest kriging variances, and cokriging with height known at the validation points incurs the least. The mean squared errors, however, are least for the autokriging. This suggests that the linear model of coregionalization does not describe the data well. One might expect this when the correlations between the properties are only moderate, as is the case for these data. The Table also shows that simple regression is a relatively poor predictor. This is partly because the correlations are moderate and partly because it takes no account of the spatial dependence in the data. Simple regression is not a satisfactory means of prediction in these circumstances.

Paul Krause has all of the mapping files of the autokriged and cokriged estimates for the properties examined. We could not prepare these maps as we did not have the outline of the relevant part of the USA. We should like to include these maps at some stage.

Table 3: Cross variogram models for the climatic data with the target variable first.

PE × height	exponent 1.2			
	Nugget variance			
		Potential transpiration	10.85	
		Square root height	25.52	60.03
	Gradient			
		Potential transpiration	31.14	
		Square root height	−7.33	5.72
Continentality	exponent 1.4			
× height	Nugget variance			
		Continentality	5.86	
		Square root height	−6.96	51.00
	Gradient			
		Potential transpiration	2.38	
		Square root height	2.49	3.44
Mrange	exponent 1.0			
× height	Nugget variance			
		Mrange	12.58	
		Square root height	2.82	39.36
	Gradient			
		Potential transpiration	8.26	
		Square root height	7.97	10.28
Temperature	exponent 1.2			
× height	Nugget variance			
		Temperature	0.60	
		Square root height	5.30	46.85
	Gradient			
		Temperature	9.40	
		Square root height	−5.25	5.80

Table 4: Summaries of kriging errors. Cokriging (121) means cokriging the target variable with data from only the 121 test sites; cokriging (121+56) means cokriging it with data from the 121 test sites plus height at the target points.

	Mean error	Mean squared error	kriging variance	Variance ratio
Height × PE				
Autokriging	−0.03	45.0	54.2	0.83
Cokriging (121)	−0.32	52.4	50.7	1.03
Cokriging (121+56)	−0.27	46.3	44.7	1.04
Regression	−1.92	804.0	887.3	0.91
Height × Continentality				
Autokriging	0.08	2.35	10.4	0.23
Cokriging (121)	0.21	2.96	9.97	0.30
Cokriging (121+56)	0.19	2.53	9.65	0.26
Regression	1.24	51.55	55.07	0.94
Height × Mrange				
Autokriging	0.18	25.31	27.13	0.93
Cokriging (121)	0.25	25.15	26.88	0.94
Cokriging (121+56)	0.24	26.21	22.57	1.16
Regression	0.91	69.35	58.09	1.19
Height × Temperature				
Autokriging	−0.16	2.35	12.50	0.19
Cokriging (121)	−0.25	2.55	12.27	0.21
Cokriging (121+56)	−0.25	2.75	11.94	0.23
Regression	−0.72	145.7	299.4	0.49

PART III: KRIGING, OPTIMAL SAMPLING AND KRIGING ANALYSIS

For this part of the analysis we return to the SPOT image of Fort Benning, Columbus, Georgia, recorded in November 1994. The pixels of the image have a resolution on the ground of about 20 m × 20 m. There are three wave bands: Green, Red and Near Infra Red (NIR). The variogram analysis of these wavebands is decribed in the final report of the first phase of the contract (N68171-95-C-9007).

In this part of the project we explored kriging using the SPOT imagery for the part of Fort Benning being studied. First we describe kriging and how it has been used to show the likely estimation variances for different sampling intensities in relation to the three wavebands. The kriging equations enable sampling schemes to be designed when the variogram is known and before collecting any data. The pixel values for channels 2 (Red, R), 3 (Infra-red, I) and for the normalized difference vegetation index, NDVI = (I - R)/(I + R), were also kriged to obtain a choropleth map. The aim of kriging pixel data is twofold: to remove some of the noise from the image and to remap the information based on isarithms chosen to match the likely reflectance of the vegetation. A more effective way of removing noise than by ordinary kriging is to filter the pixel information by a kriging analysis. In the previous project we detected two marked scales of spatial variation in the image from the variogram analysis. The variogram showed that there was a short-range variation of about 9 pixels long (180 m) and a much longer one of about 150 pixels (3 km). We filtered the image according to these spatial scales by kriging the short and the long spatial components independently.

The theory of kriging and its relation to optimal sampling is described (Journel & Huijbregts, 1978; Burgess & Webster, 1980; Webster & Oliver, 1990), and the theory of the kriging analysis to filter data is also given (Goovaerts & Webster, 1994).

Theory

We assume a simple model of a spatially correlated random variable:

$$Z(\mathbf{x}) = \mu + \varepsilon(\mathbf{x}) , \tag{8}$$

where μ is the mean of the process, and $\varepsilon(\mathbf{x})$ is another random variable with a mean of zero and variogram $\gamma(\mathbf{h})$, where $\mathbf{h}$ is the lag.

We also assume the intrinsic hypothesis, namely that the expected differences between the values at $\mathbf{x}$ and $\mathbf{x} + \mathbf{h}$ is 0 and their variance depends only on $\mathbf{h}$. In those circumstances $\gamma(\mathbf{h})$ is also the variogram of $Z(\mathbf{x})$.

Characteristics of kriging

At its simplest kriging is a method of local weighted moving averaging of the observed values within a neighbourhood V. Weights are allocated to the sample data within

the neighbourhood of the point or block to be estimated. The weights depend on the structure of the variation of the $Z(\mathbf{x})$, defined by the variogram model, and the configuration of the sampling sites. The weights are allocated so as to minimize the estimation variance, or kriging variance, and the estimates are unbiased. Hence, in this sense, kriging is an optimal estimator. Kriging is also an exact interpolator in the sense that the kriged value at a sampling site is the observed value there, and the estimation variance is zero. Kriging can be done at points or over areas (blocks). In the analysis that we report here we regarded each pixel in the image from Fort Benning as a point and used punctual kriging.

In the usual situation a kriged estimate, $\widehat{Z}(\mathbf{x}_0)$, is a weighted average of data, $z(\mathbf{x}_1), z(\mathbf{x}_2), \ldots, z(\mathbf{x}_n)$:

$$\widehat{Z}(\mathbf{x}_0) \quad = \quad \sum_{i=1}^{n} \lambda_i z(\mathbf{x}_i) \ , \tag{9}$$

where λ_i are the weights.
To ensure that the estimates are unbiased the weights are made to sum to 1:

$$\sum_{i=1}^{n} \lambda_i z(\mathbf{x}_i) \quad = \quad 1 \ .$$

We also want to minimize the estimation variance, which is given by

$$\begin{aligned} \mathrm{var}[\widehat{Z}(\mathbf{x}_0)] \quad &= \quad \mathrm{E}[\{\widehat{Z}(\mathbf{x}_0) - Z(\mathbf{x}_0)\}^2] \\ &= \quad 2\sum_{i=1}^{n} \lambda_i \gamma(\mathbf{x}_i, \mathbf{x}_0) - \sum_{i=1}^{n}\sum_{i=j}^{n} \lambda_i \lambda_j \gamma(\mathbf{x}_i, \mathbf{x}_j) \ , \end{aligned} \tag{10}$$

where $\gamma(\mathbf{x}_i, \mathbf{x}_j)$ is the semivariance of Z between points $\mathbf{x}_i$ and $\mathbf{x}_j$, and $\gamma(\mathbf{x}_i, \mathbf{x}_0)$ is the semivariance between the ith datum and the point for which the estimate is required.

In ordinary kriging the mean of the random variable, μ, is unknown. The estimation variance of $Z(\mathbf{x}_0)$ is minimized, subject to the non-bias condition, when

$$\begin{aligned} \sum_{i=1}^{n} \lambda_i \gamma(\mathbf{x}_i, \mathbf{x}_j) + \psi(\mathbf{x}_0) \quad &= \quad \gamma(\mathbf{x}_j, \mathbf{x}_0) \ \text{ for all } \ j \\ \sum_{i=1}^{n} \lambda_i \gamma(\mathbf{x}_i) \quad &= \quad 1 \ . \end{aligned} \tag{11}$$

These are the kriging equations. The quantity $\psi(\mathbf{x}_0)$ is a Lagrange multiplier, which is introduced to achieve the minimization. The kriging variance is then obtained from

$$\sigma_{\mathrm{e}}^2 \ = \ \sum_{i=1}^{n} \lambda_i \gamma(\mathbf{x}_i, \mathbf{x}_0) + \psi(\mathbf{x}_0) \ . \tag{12}$$

Optimal sampling

The estimation variance for kriging depends only on the variogram and the configuration of sampling points and not on the measured values. This means that if the variogram is known then the estimation variances can be determined for any desired sampling configuration *before* the sampling is done. Therefore, we should be able to design a sampling scheme to meet a specified tolerance or precision for a property. We may or may not have data at this stage. In this case we had the image data, but for field work or to sample the image for data compression we want to minimize the ground-based sampling or the number of data retained according to the estimation variance (the square of the standard error) that we can tolerate.

We had determined the models for the variograms previously. They were all isotropic double exponential, with equation

$$\gamma(\mathbf{h}) \;=\; c_0 + c_1\{1 - \exp(-h/a_1)\} + c_2\{1 - \exp(-h/a_2)\}\;, \qquad (13)$$

in which c_0 is the nugget variance, c_1 and c_2 are the sills of the short-range and long-range components respectively, and a_1 and a_2 are the corresponding distance parameters. The values of the parameters are given in Table 5. Using these models we formed the punctual kriging system, Equations (11), and solved it to determine the punctual kriging variances by Equation (12) at the centres of square grid cells of side 2, 3, ..., pixels. These are the largest variances associated with the reconstruction of the images from sampling at the intervals 2, 3, ..., pixels.

One might wish to discover the minimum number of pixels to retain and still maintain a sufficiently small error, an acceptable tolerance. For this we plotted the estimation variances against grid spacing for the three wavebands, Figure 1, from which the sample spacing can be read for any specific tolerance.

We do not know what error is tolerable in this instance. Nevertheless, from the graphs it is clear how the estimation variance increases rapidly with increased sample spacing, or equivalenty a smaller sample. For data compression, which we deal with in Part IV of this report, the graphs illustrate at the outset the kind of estimation variances or standard errors that we shall incur by removing information.

Results of optimal sampling analysis

Channel 1

The graph of the estimation variances plotted against grid spacing in numbers of pixels for channel 1 has a very steep initial slope. This results from the short-range component of the variogram. The pixel map of channel 1 shows that the short range variation is dominant. If a variance of 50 is chosen for the tolerance, which is 62.5% of the upper limit of the variance in this graph, then a sampling interval of 9 pixels

would be needed. Hence, estimates based on this sampling interval would have a considerable error even though the sampling interval or reduction in data would be fairly small. For the vegetation survey in the previous project we recommended a minimum sampling interval of 150 m (7.5 pixels) which would give an estimation variance of about 38, about 50% of the total variance. With a sampling interval of more than 60 pixels (1500 m) for channel 1, which was the maximum sampling interval, we recommended for sampling the long-range component there would be little spatial dependence in the data. This graph confirms our earlier recommendations. It also shows the importance of an objective approach to sampling for interpolation or data reduction.

Channel 2

The initial slope of this graph is also steep. At larger dsitances it becomes more gradual. The variances this time are for the data transformed to logarithms. The short- and long-range components are both important for this waveband. The pixel map of this channel appears less noisy than that of channel 1. For a spacing of 7.5 pixels the estimation variance would be 30%, and for one of 45 pixels 60%.

Channel 3

This graph has the gentlest slope, although it is still steep near to the origin because of the short-range component of the variation. A sampling interval of 7.5 pixels would result in an estimation variance of 30% of the total, whereas for a 50-pixel sampling interval it would be 60% for the long-range component.

Channels 2 and 3 (Red and Near Infra Red) are the ones we expect to be most closely related to the vegetation. They are also similar to each other and express a similar degree of variation.

Summary

Figure 1 shows the maximum estimation variances that would result when reconstructing images from sampling the image for data reduction. Clearly it depends on the variation in the data. These graphs also show the effect of the two scales of variation on the sampling interval needed to resolve the variation present.

Table 5: Variogram model parameters for the three channels and NDVI

Channel	c_0 variance	c_1 variance	c_2 variance	a_1 pixels	a_2 pixels
1 – rows	0	35.74	43.95	2.83	28.61
– columns	0.88	44.92	45.92	3.76	61.67
– average	0	40.84	42.71	3.26	38.87
2 – rows	0	0.0213	0.0904	2.19	44.67
– columns	0	0.0329	0.0854	4.49	79.00
– average	0	0.0262	0.0845	3.23	53.36
3 – rows	0	0.0105	0.0467	1.76	52.91
– columns	0	0.0130	0.0335	3.03	52.47
– average	0	0.0115	0.0400	2.33	51.92
NDVI					
– rows	0	0.00406	0.00942	4.51	70.45
– columns	0	0.00422	0.00569	5.24	38.85
– average	0	0.00428	0.00725	5.06	55.80

NB: The distance parameters of the double exponential models fitted to the variograms can be multiplied by 3 to obtain the approximate ranges of spatial dependence.

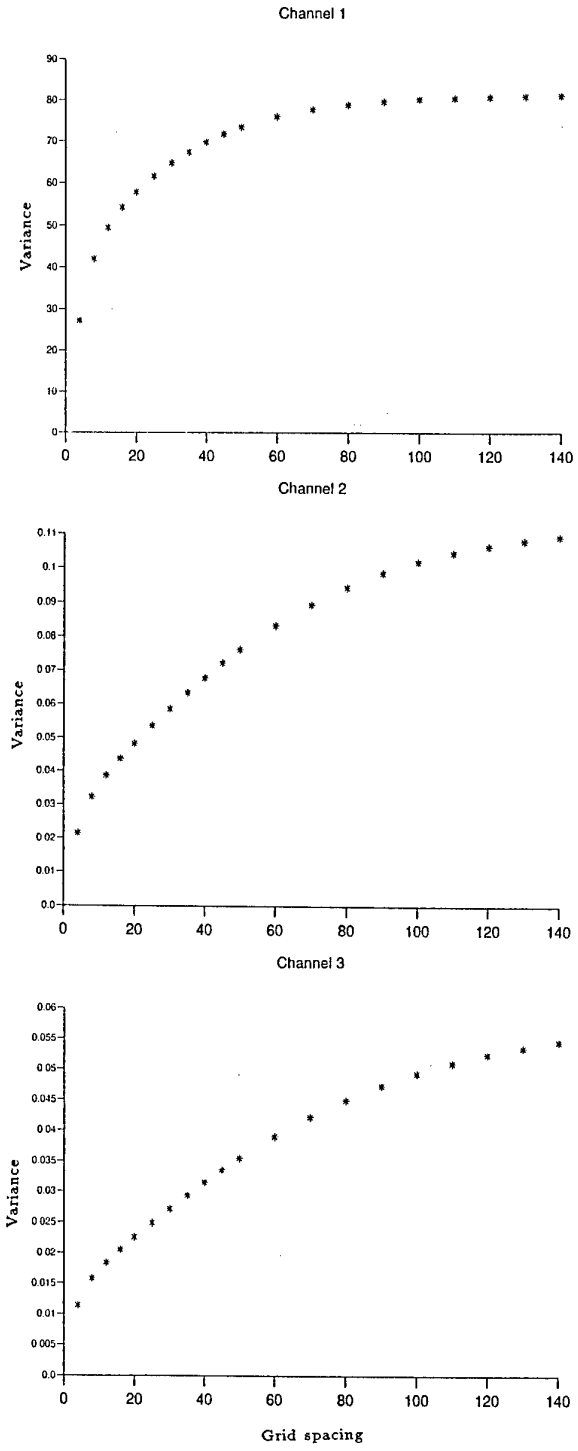

Figure 1: Graphs of estimation variance against sampling interval for Channel 1 (Green); Channel 2 (Red) and Channel 3 (Infra-red).

Kriging

For this part of the project we examined the best way of smoothing or removing noise from the pixel information for mapping. The simplest approach was to use ordinary kriging for the digitial numbers (DNs) of channels 2 and 3 and for NDVI (the normalized difference vegetation index). We used the double exponential models of the raw data for each of these variables and kriged the raw data on a grid that was offset by 0.5 of a pixel in both the north-south and east-west dimensions; this was to avoid estimating at the data points, which would have been pointless. We used the raw data rather than the transformed values so that TEC can make comparisons between the isarithmic intervals and the DNs for the classes of vegetation. We kriged at intervals of both 1 and 2 pixels. We drew only the maps of the latter estimates because there was little benefit in using the more detailed estimates.

Results of ordinary kriging

For channels 2 and 3 (R and I, respectively), Figures 2 and 3, the isarithmic intervals were chosen to correspond with the average reflectance for the different classes of vegetation suggested by TEC. This was more straightforward for channel 2 because the spectral values seemed to match those of the vegetation closely. This waveband also had the largest correlation with the vegetation values when they were compared in the previous project. The reflectance values associated with the ground cover classes for Channel 2 are given in Table 6.

The general appearance of the maps for Channels 2 and 3 is similar, especially for the large reflectance values over the open spaces and roads. The major differences in the pattern are in the south west. Here there appear to be differences in the short-range variation picked up by the different sensors. In both cases the swampy areas associated with the Ochillee Creek show up clearly with the blue shading. Also King's Pond is clearly visible on both maps (Figures 2 and 3).

The map for NDVI (Figure 4) is somewhat different from the others: the areas of large reflectance (small NDVI) are more clearly defined. It appears to contain more detail of the variation. The map is more similar to that of Channel 3 than that of Channel 2, suggesting that NDVI reflects the pattern in the Infra-red rather more than that in the red. This is more apparent in the southern part of the region, Figures 2 to 4. For Channel 3 and NDVI the western and eastern halves of the map appear very different. The difference seems to be physiographic, with the boundary following approximately the western edge of the Branch valley.

In all of the kriged maps the short- and long-range components of the variation are clearly visible. These maps need to be validated now against the field data that were collected in the Autumn of 1995 by TEC. We did not have these data for comparison. It now remains for the team at TEC to compare the kriged maps with the ones of

Table 6: Average reflectance values associated with ground cover class for channel 2

Ground cover class	Reflectance Value
Water	24.0
Pine/Hardwood Wet	25.0
Hardwood/Pine and hardwood	25.9
Brush	26.1
Pine/Hardwood	26.3
Hardwood Wet	26.5
Pine/Plantation	27.0
Longleaf Pine	28.0
Oak/Pine	28.5
Open space	30.0

the classification of ground cover to see which is better for predicting ground cover.

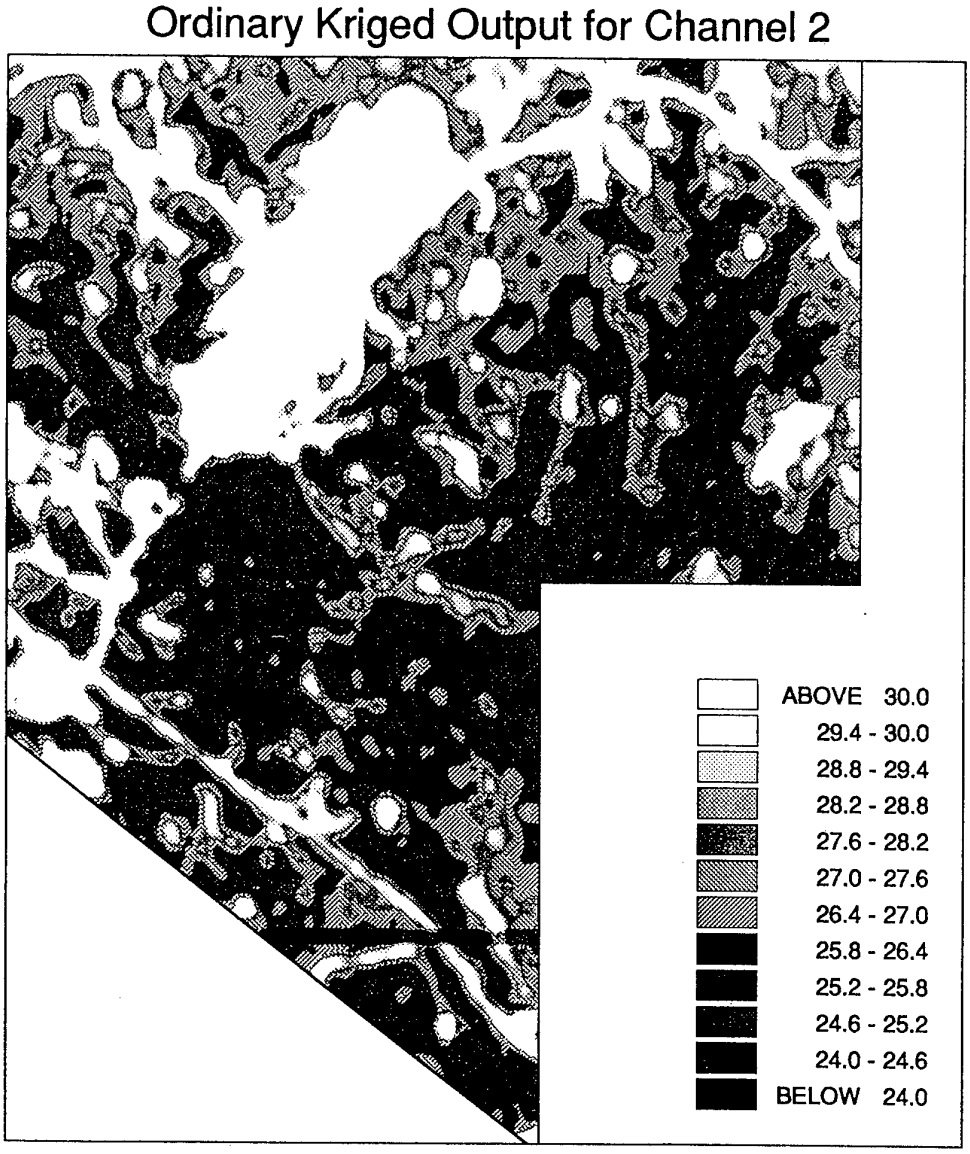

Figure 2: Map of ordinary kriged estimates for the Fort Benning study area: Channel 2.

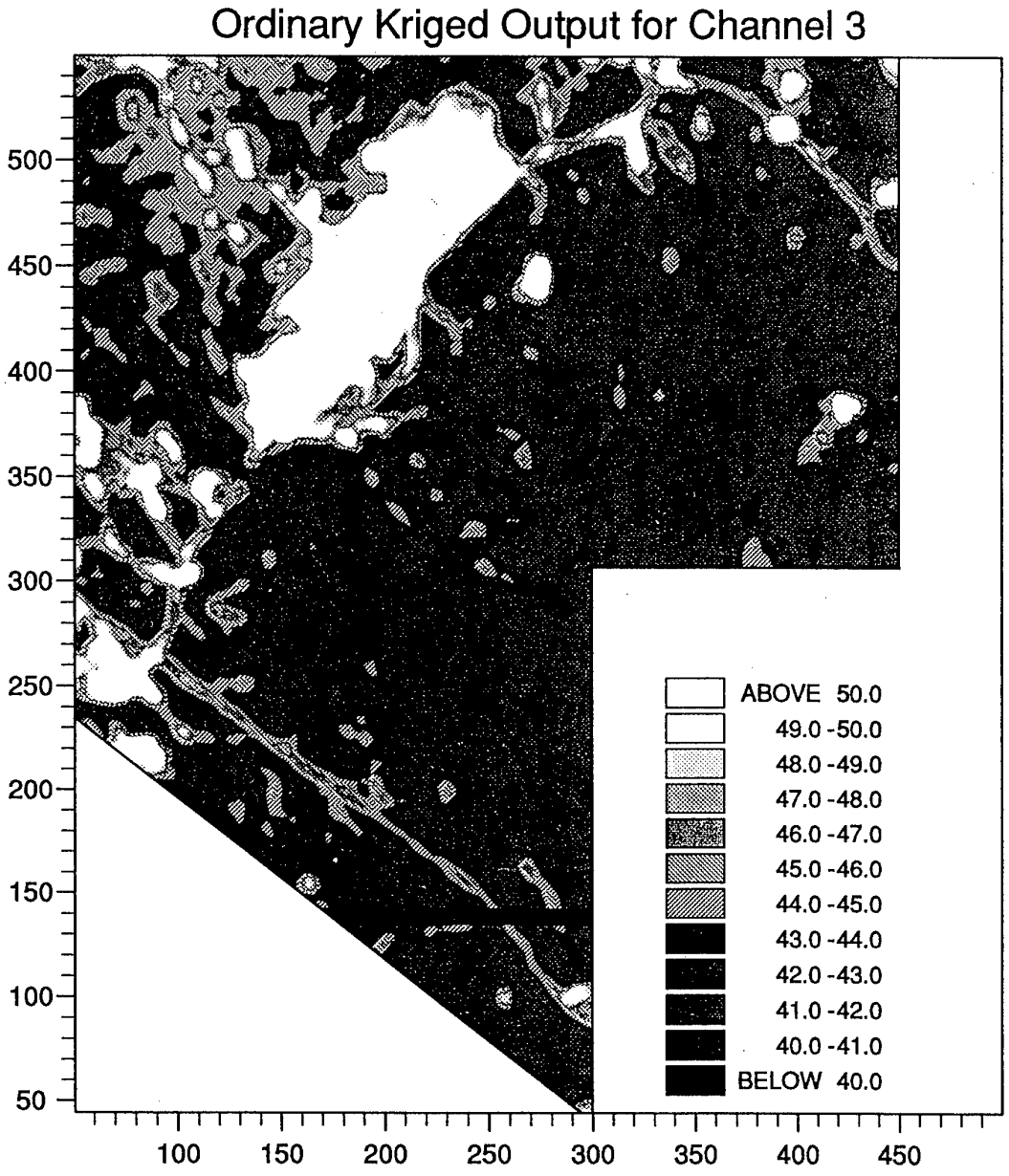

Figure 3: Map of ordinary kriged estimates for the Fort Benning study area: Channel 3.

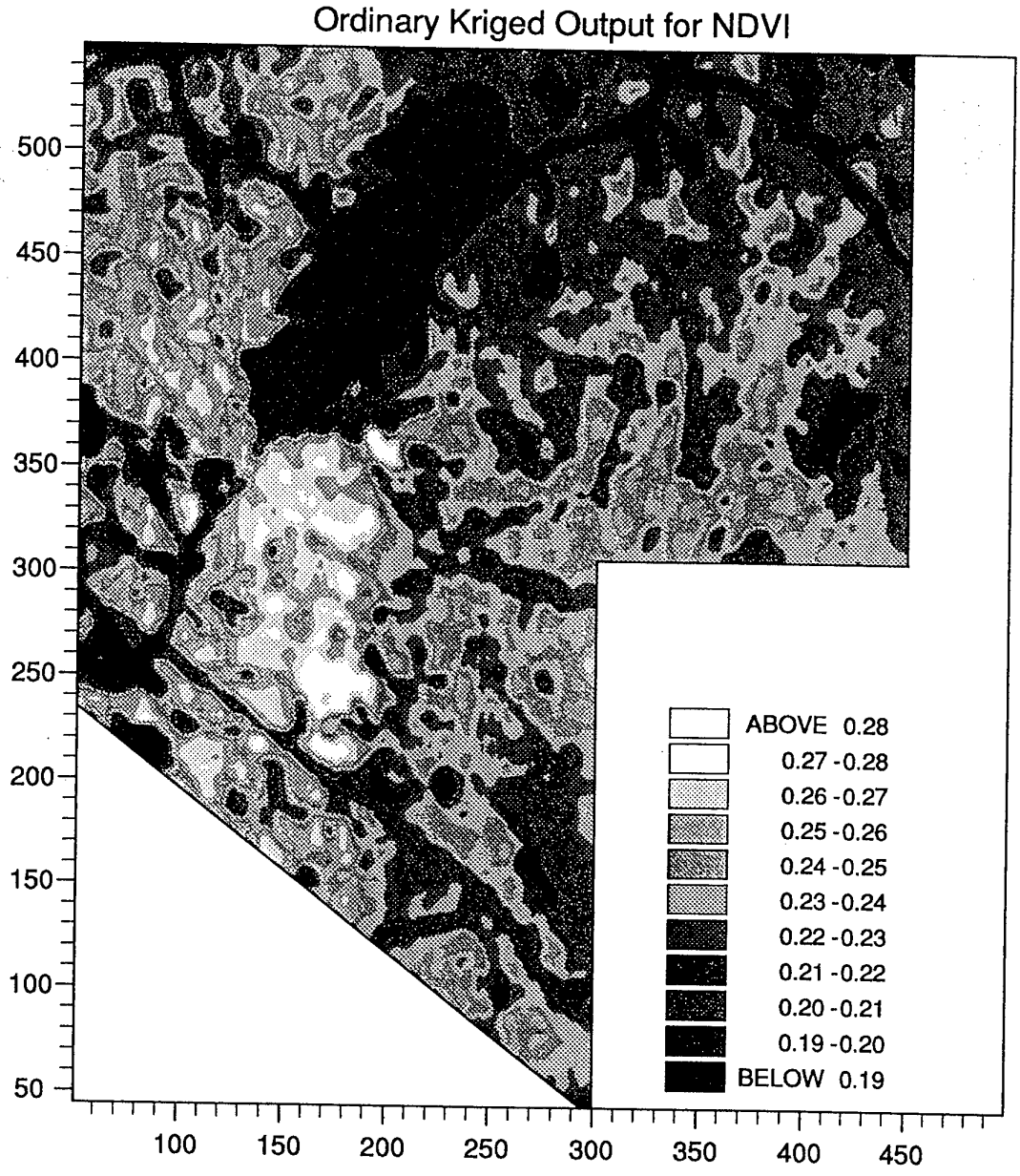

Figure 4: Map of ordinary kriged estimates for the Fort Benning study area: NDVI.

Kriging analysis

The variogram may be just one simple structure, or it may be the sum of two or more structures, one nested inside the other, and each with its own scale, thus

$$\gamma(\mathbf{h}) \;=\; \gamma^1(\mathbf{h}) + \gamma^2(\mathbf{h}) \ldots \;, \tag{14}$$

where the superscripts refer to the separate structures. This matches the real world in which factors such as relief, geology, tree-throw, fauna, and man's divisions into fields and farms operate on their own characteristic spatial scales.

If we assume that the processes are uncorrelated then we can represent Equation (14) by the sum of K basic variograms:

$$\gamma(\mathbf{h}) \;=\; \sum_{k=1}^{K} b^k g^k(\mathbf{h}) \;, \tag{15}$$

where $g^k(\mathbf{h})$ is the kth basic variogram function and b^k is a coefficient that measures the relative contribution of $g^k(\mathbf{h})$ to the sum. This then is our linear model of regionalization.

Identifying the spatial structures.

When we know that there are nested structures present we can attempt to identify them separately. We first computed the experimental variograms from the raw data for this analysis using the usual estimator. We fitted a nested model with two exponential functions, Equation (13), but without the nugget.

Kriging analysis: theory.

Once distinct spatial structures have been identified in the variogram we can try to separate their sources. This is effectively filtering. It enables us to isolate specifically local or regional sources of variation and, thereby, interpret them more easily than when they are combined. For complex imagery separating out the different sources of variation helps to show the spatial structure present at the different scales, and it reduces the noise (Bourgault & Marcotte, 1993; Goovaerts & Webster, 1994; Wen & Sinding-Larsen, 1997). It is done by what Matheron (1982) called 'kriging analysis', and it is based on the decomposition of $Z(\mathbf{x})$ into the sum of K separate orthogonal random functions $Z^k(\mathbf{x}), k \;=\; 1, 2, \ldots, K$, each with its basic variogram $g^k(\mathbf{h})$ of Equation (15):

$$Z(\mathbf{x}) \;=\; \sum_{k=1}^{K} Z^k(\mathbf{x}) + \mu \;, \tag{16}$$

such that

$$\mathrm{E}[Z^k(\mathbf{x})] \;=\; 0$$

and

$$\frac{1}{2}\mathrm{E}[\{Z^k(\mathbf{x}) - Z^k(\mathbf{x}+\mathbf{h})\}\{Z^{k'}(\mathbf{x}) - Z^{k'}(\mathbf{x}+\mathbf{h})\}] = b^k g^k(\mathbf{h}) \quad \text{if} \quad k = k'$$
$$= 0 \quad \text{otherwise} . \qquad (17)$$

Relation (17) expresses the mutual independence of the K random functions $Z^k(\mathbf{x})$. With this assumption, the nested model (15) is easily retrieved from relation (16). We assume that $Z(\mathbf{x})$ is second-order stationary, which accords with the results above (the variogram models have asymptotes). The $Z^k(\mathbf{x})$ are the spatial components, and they represent the behaviour of $Z(\mathbf{x})$ at the spatial scales defined by the distance parameters of the basic variogram functions, $g^k(\mathbf{h})$. In practice each spatial component is estimated as a linear combination of the observations $z(\mathbf{x}_i)$:

$$\widehat{Z}^k(\mathbf{x}_0) = \sum_{i=1}^{n} \lambda_i^k z(\mathbf{x}_i) , \qquad (18)$$

where n is the number of observations, $z(\mathbf{x}_i), i = 1, 2, \ldots, n$, used for the estimation, and the λ_i^k are the weights assigned to the observations.

The n weights are chosen to ensure that the estimate is unbiased and that the estimation variance is minimal. This leads to the kriging system:

$$\sum_{j=1}^{n} \lambda_j^k \gamma(\mathbf{x}_i, \mathbf{x}_j) - \psi = b^k g^k(\mathbf{x}_i, \mathbf{x}_0) \quad \text{for all} \quad i = 1, 2, \ldots, n ,$$
$$\sum_{j=1}^{n} \lambda_j^k = 0 . \qquad (19)$$

This system is is solved to find the weights, λ_i^k, to insert into Equation (18). The quantity ψ is a Langrange multiplier. From Equation (16), $\mathrm{E}[Z^k(\mathbf{x})] = 0$, and so the weights sum to 0 to assure unbiasedness, not to 1 as in the ordinary kriging formulation, system (11).

To account for local non-stationarity the kriging is usually done in fairly small moving neighbourhoods centred on $\mathbf{x}_0$. Then it is necessary only that $Z(\mathbf{x})$ is locally stationary, or *quasi-stationary*, so that Equation (16) can be rewritten as

$$Z(\mathbf{x}) = \sum_{k=1}^{K} Z^k(\mathbf{x}) + \mu(\mathbf{x}) , \qquad (20)$$

where $\mu(\mathbf{x})$ is a local mean which can be considered as a long-range spatial component.

Estimation of the long-range component, i.e. the local mean $\mu(\mathbf{x})$ and the spatial component with the largest range, can be affected by the size of the moving neighbourhood (Galli *et al.*, 1984). To estimate a spatial component with a given range,

the diameter of the neighbourhood should be at least equal to that of the range. It frequently happens when the sampling density and the range are large that there are so many data within the chosen neighbourhood that only a small proportion of them is retained. Although modern computers can handle many data at a time, the number of data used must be limited to avoid instabilities when inverting very large covariance matrices. Further, even if all the data could be retained, only the nearest ones contribute to the estimate because they screen the more distant data. Consequently, the neighbourhood actually used is smaller than the neighbourhood specified, which means that the range of the estimated spatial component is smaller than the range apparent from the structural analysis. Galli *et al.* (1984) recognized this, and where data lie on a regular grid they proposed using only every second or every fourth point to cover a large enough area but still with sufficient data. Such selection is somewhat arbitrary, and we have adopted an alternative proposed by Jaquet (1989) which involves adding to the long-range spatial component the estimate of the local mean.

Results of the kriging analysis: filtering

Short range

For Channel 2 (R), Figure 5, the intricate local variation associated with erosion in the area of McKenna Hill shows clearly. This area reflects much of the light because it has been cleared of vegetation. The roads are also distinct, as is other land that has been cleared. The short-range variation in the vegetation is also evident. There appear to be two main classes of reflectance, but this depends to some extent on the class intervals chosen. Essentially this map shows the main local changes and where these can be expected from one ground cover class to another. It is not possible to say what the type of cover is from this map at present.

The map, Figure 6, for Channel 3 (I) shows more detail in the short-range variation. However, McKenna Hill does not stand out as clearly. There are now three main reflectance groups in the vegetation. Further field work would be needed to gain insight into their precise meaning. What is apparent is that the swamp in the central part of the image is not evident at this scale, but the local variation within it is.

The short-range map for NDVI, Figure 7, looks like a mixture of the maps for R and I. However, there is more detail in the vegetated areas.

Long range

The long-range structures in the three maps, Figures 8 to 10, are clear. Kriging with the long-range filter evidently removes the local noise and shows the extent of the major ground cover classes. These maps differ from one another in the finer detail,

but McKenna Hill and the roads stand out in all. Channels 2 and 3 both pick out the wet areas in the central part of the maps. The yellow areas on Figure 10 for NDVI represent the wet areas, but they appear to be more extensive than in the other two maps.

Summary

There is considerable detail evident on the maps of the long-range component, and from the point of view of environmental management at the broad scale these maps should eanble a manager to identify areas for monitoring or more detailed study. The short-range maps could be of military value in that they show the amount of change in ground cover to be expected at the local scale. The difference in these scales is an order of magnitude. The local scale is around 150 m to 300 m and the long-range 1.5 km to 3 km. These maps also reflect the kinds of spatial scale of variation established from the image data in the first project and in the vegetation classes from the transects. Final interpretation of these results will depend on further information from TEC about ground cover.

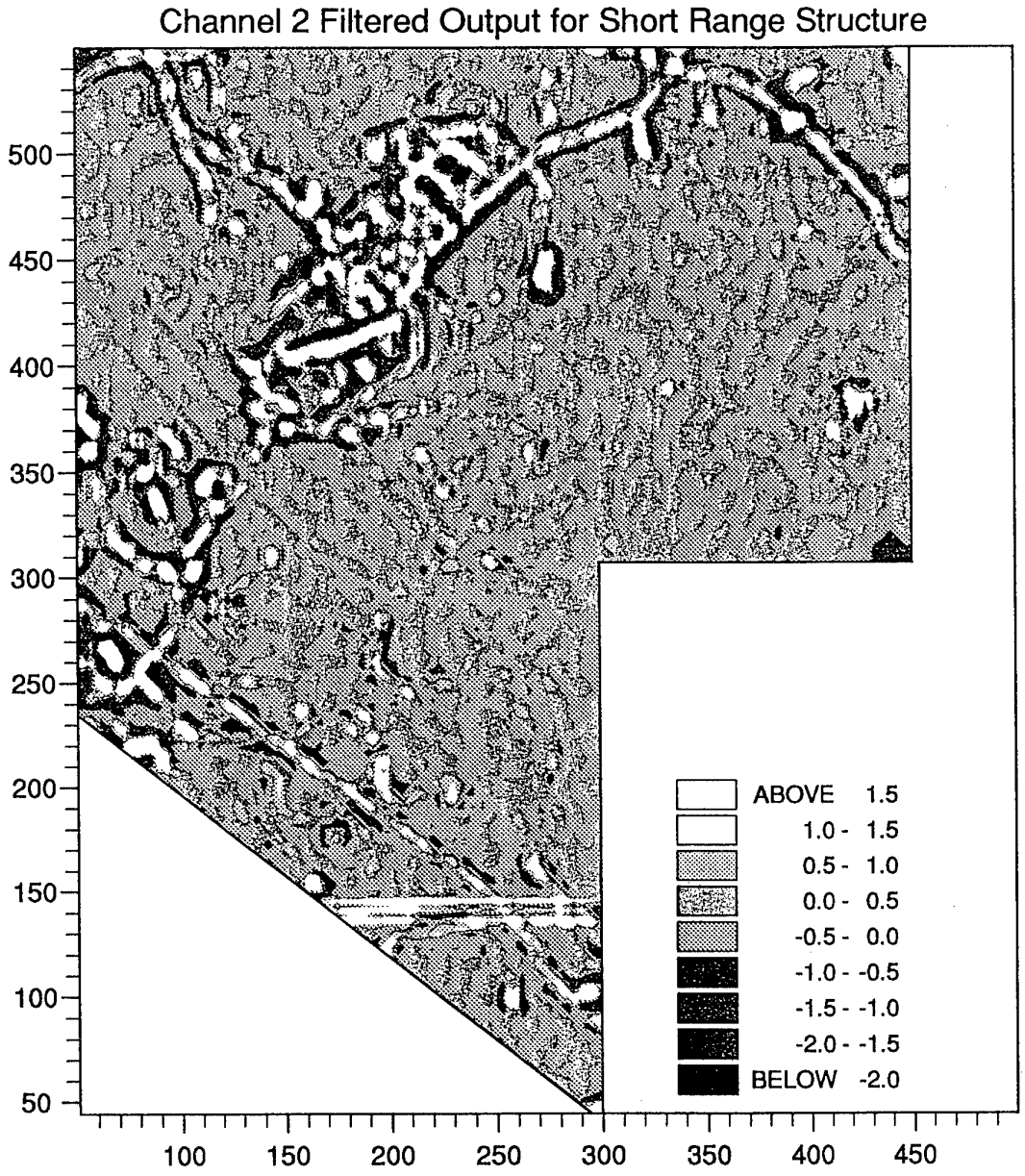

Figure 5: Map of short range kriged estimates after filtering for the Fort Benning study area: Channel 2.

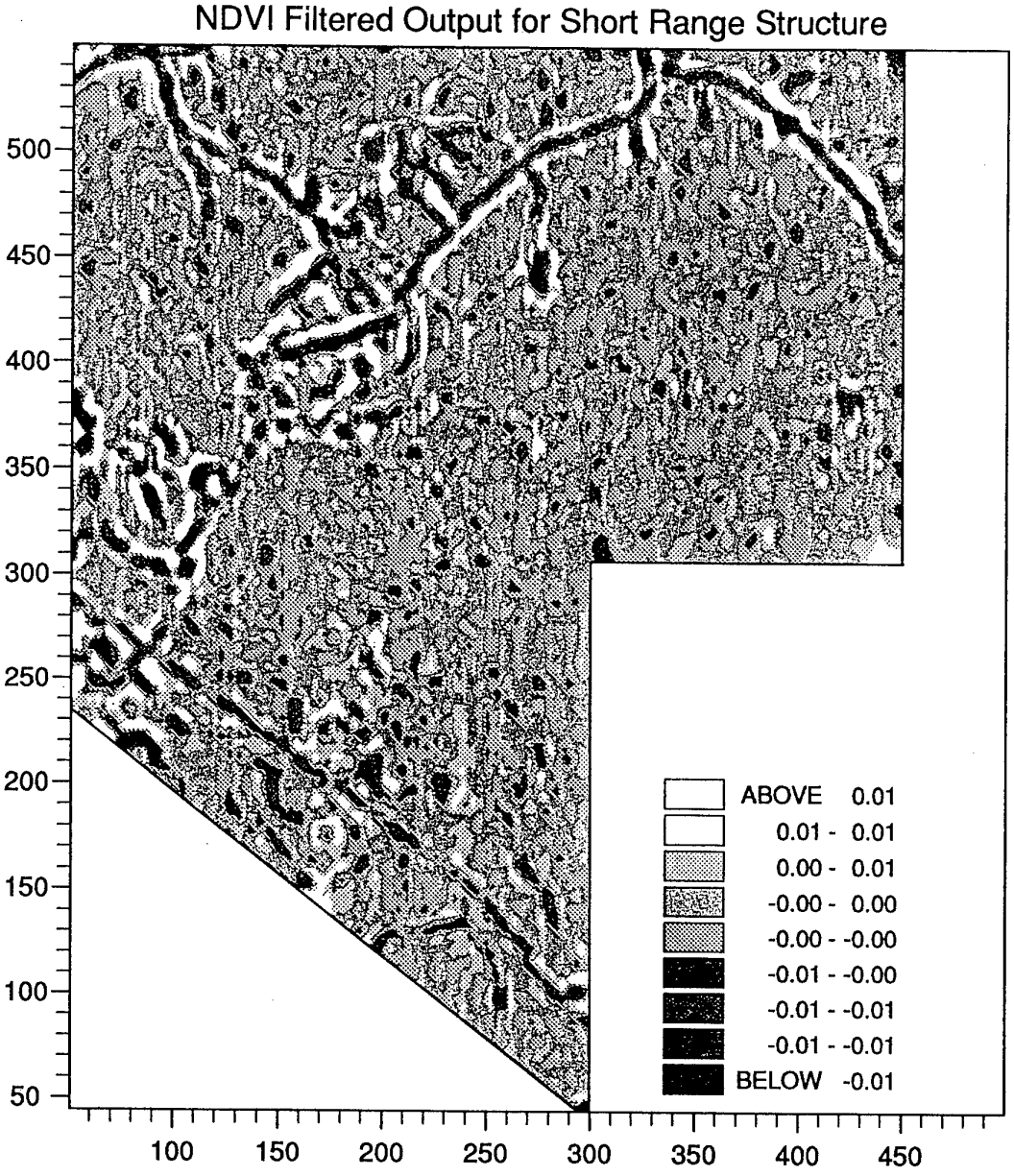

Figure 6: Map of short range kriged estimates after filtering for the Fort Benning study area: NDVI.

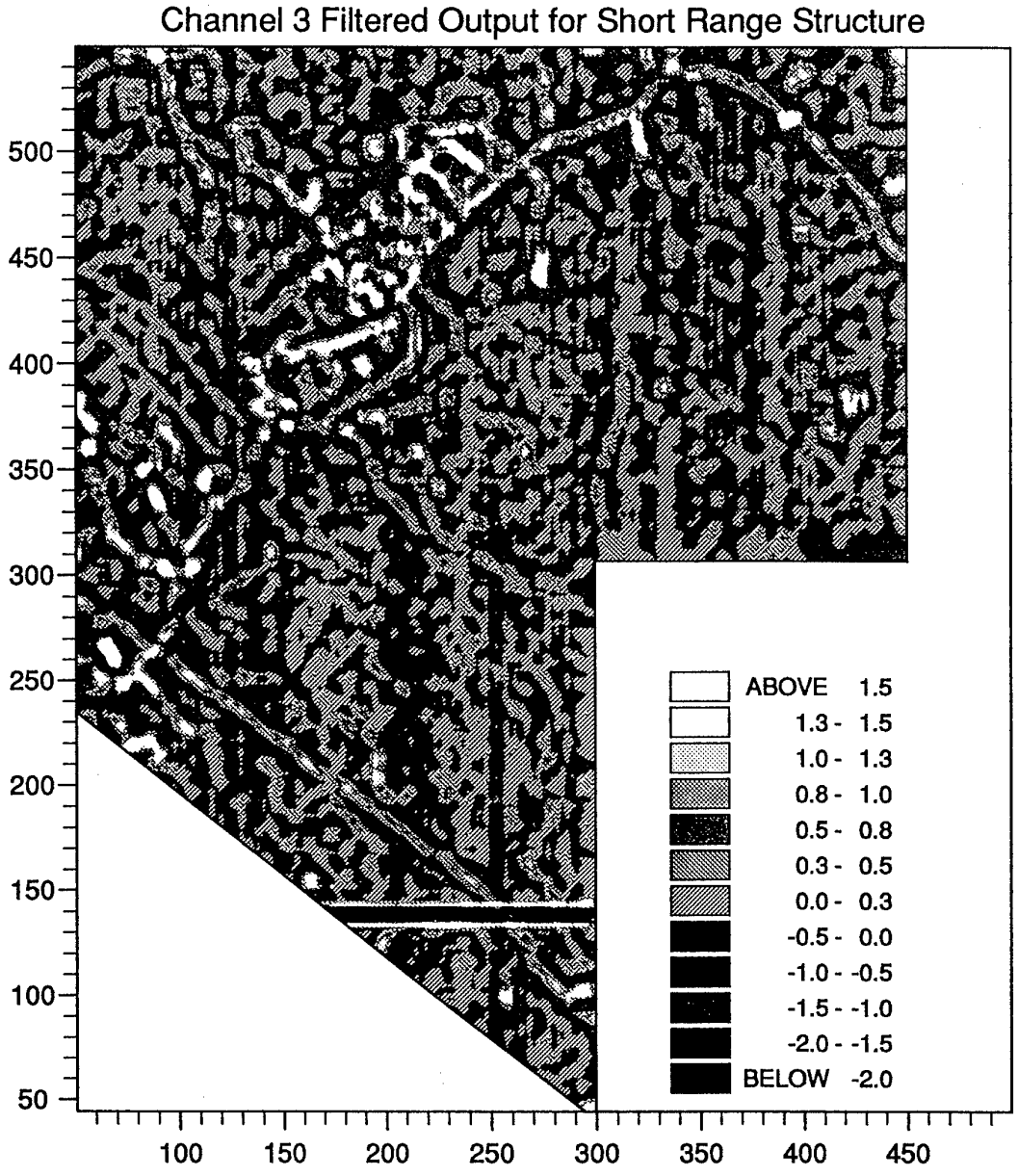

Figure 7: Map of short range kriged estimates after filtering for the Fort Benning study area: Channel 3.

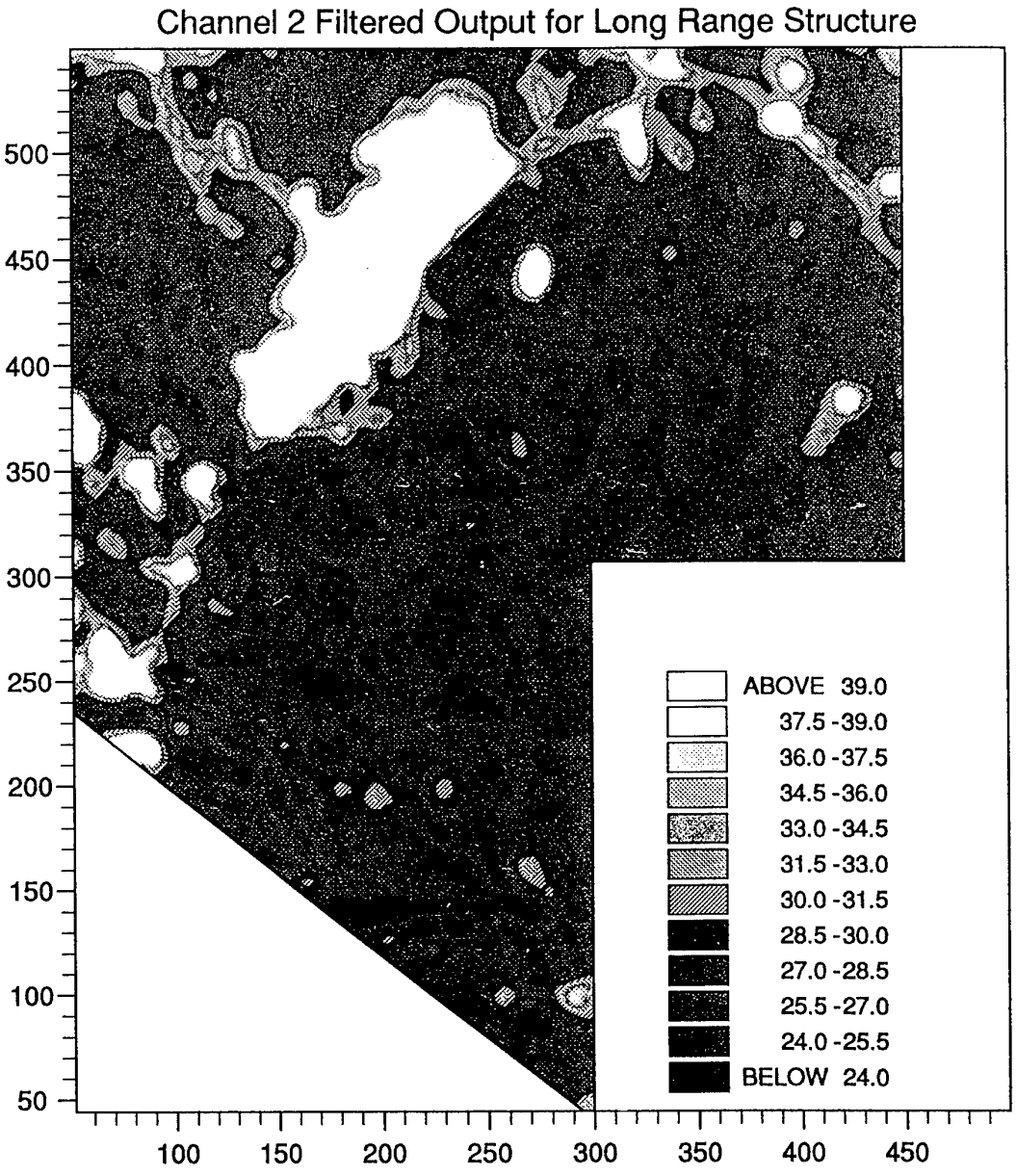

Figure 8: Map of long range kriged estimates after filtering for the Fort Benning study area: Channel 2.

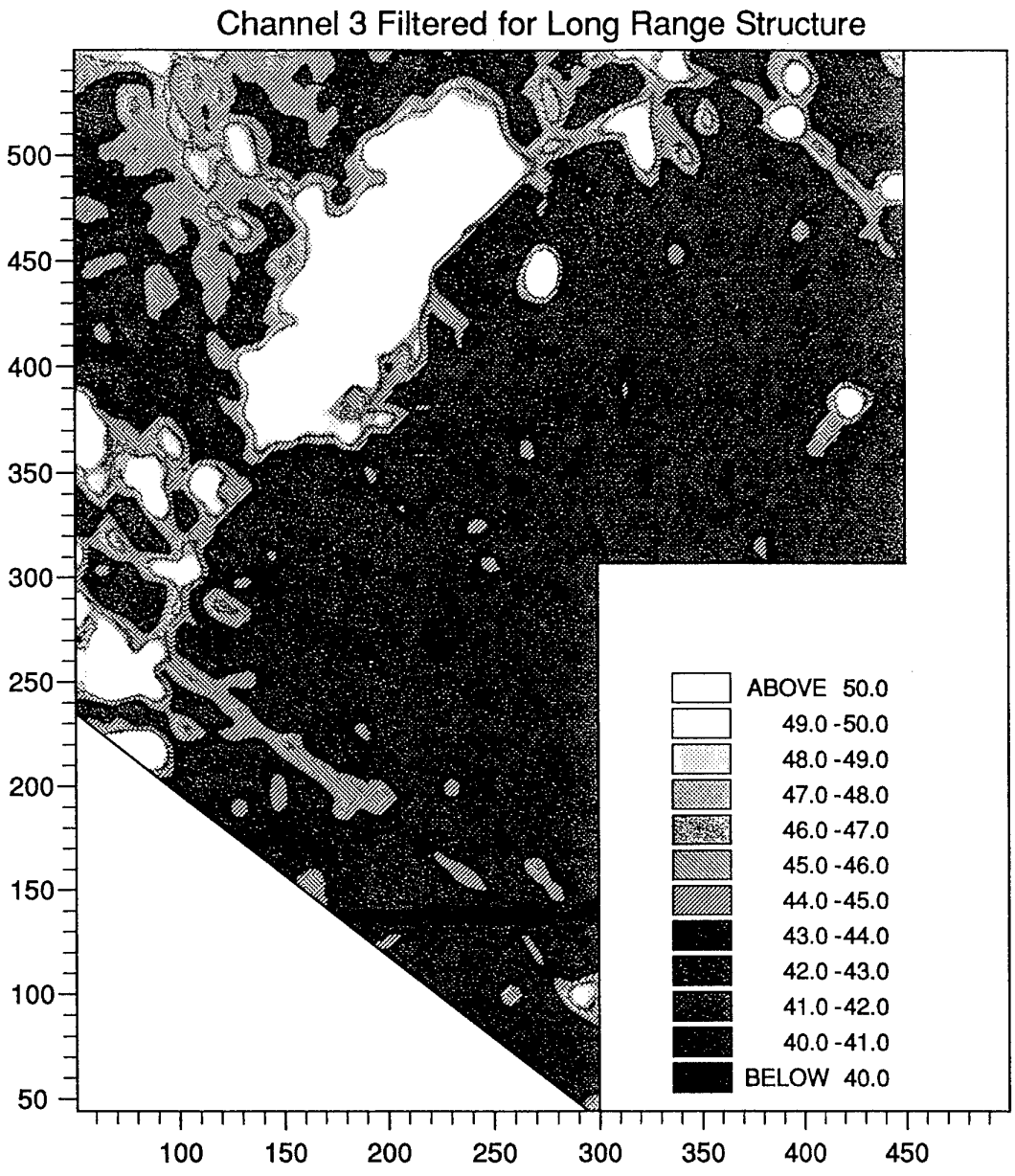

Figure 9: Map of long range kriged estimates after filtering for the Fort Benning study area: Channel 3.

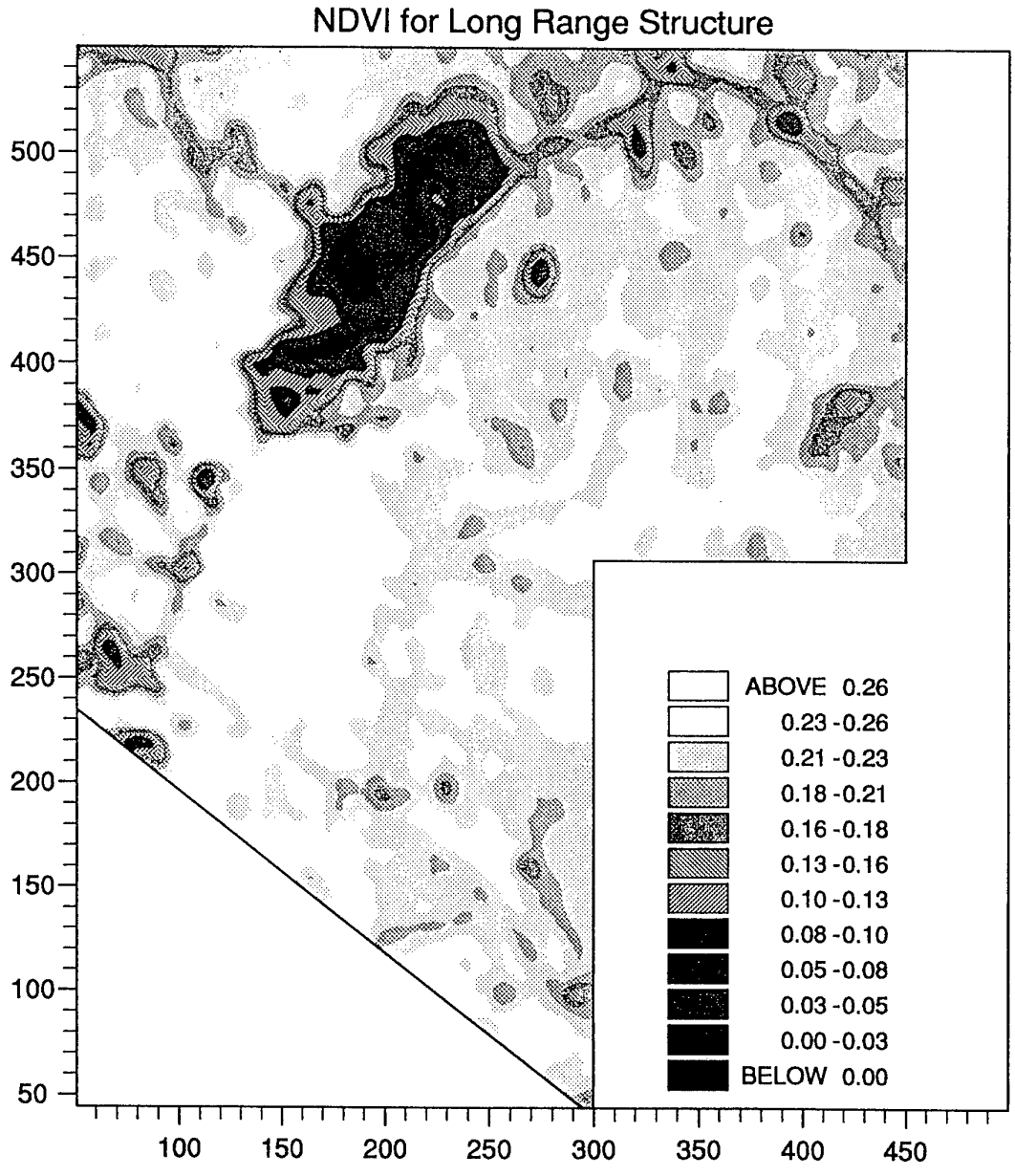

Figure 10: Map of long range kriged estimates after filtering for the Fort Benning study area: NDVI.

PART IV: DATA COMPRESSION ANALYSIS

For this part of the project we chose a part of the Fort Benning image that we had been working on. It is in the eastern part of the area: the bottom left corner is at 300 350 and the top right corner at 400 450. We have called it 'Benncut'. It is square with a side of 100 pixels. Since we wanted to compare several sets of results we decided to work with the red channel (2) only. Figure 11 shows the pixel map for this channel. We first computed the experimental variogram over all directions—this was feasible because we had reduced the number of data points sufficiently to 10 000. We then fitted a model by the usual least squares approximation. The model that fitted best was the nested spherical function. The model parameters are given in Table 7. The short-range scale of variation is similar to that for the whole region. The long-range structure is shorter than that in the region as a whole: it is 24 pixels (480 m) compared with approximately 3 km for the whole area. This suggests that there are more scales of variation nested within the image than were apparent from the initial analysis. This raises some interesting ideas on the relations between different spatial scales for different sizes of area. This is something that we hope to pursue in future.

For each kriging and simulation (see below) we divided the 10 000 points in Benncut into two groups. One contained the data from which to krige and which would serve as conditioning data for simulation. The other contained the remainder of the pixels at which we should krige or simulate to reconstruct the image and the values that we should use to validate the result. We reduced the number of data points in the first of the files in stages as shown in Table 8.

Table 7: Parameters of the double spherical variogram model for Benncut

	Variance			Distance/pixels	
Channel	c_0	c_1	c_2	a_1	a_2
2 – raw	0.3107	1.3501	0.9566	6.898	24.45
– scores	0.1711	0.3862	0.4561	7.005	21.30

Table 8: The order of data reduction.

Order of reduction	Number of conditioning data	Percentage retained	Number of validation data
1 in 2 × 2	2500	25	7500
1 in 3 × 3	1122	11.22	8878
1 in 4 × 4	625	6.25	9375
1 in 5 × 5	400	4	9600
1 in 6 × 6	272	2.72	9728
1 in 7 × 7	210	2.1	9790

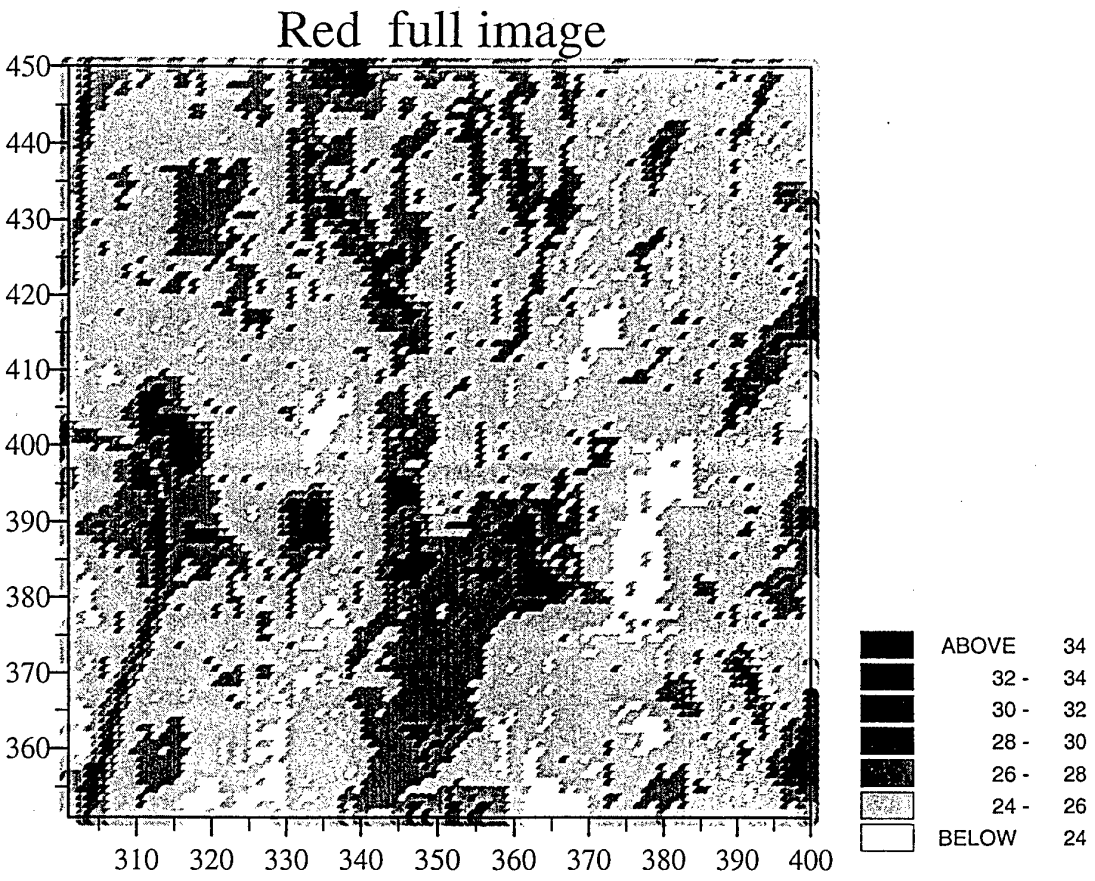

Figure 11: Pixel maps of digital numbers for channel 2 for Benncut

Ordinary kriging. This is the method of estimation embodied in geostatistics that is described in Part III. The selected data were used in conjunction with the variogram model in Table 7 to estimate the DN values of the red channel. This was done for each of the seven files in Table 8, and the resulting estimates were mapped, Figures 12, 14, 16, 18, 20, and 22.

Sequential Gaussian Simulation. This is a method of stochastic simulation that adheres to the theory of regionalized variables. The basic aims of simulation are to generate 'data' with the same spatial structure as those from which the real data are thought to arise. The results may be conditioned by existing data so that they never depart grossly from the actual situation. The values at data points are retained, so that the simulated surface passes through them. Simulation is different from kriging, and incidentally from most other forms of interpolation in that it attempts to retain the spatial structure, whereas kriging smoothes as it attempts to find the best local estimate of $Z(\mathbf{x})$ at each unsampled location by minimizing the estimation variance. Kriging thus loses variance. In simulation the global features that result, such as the overall texture of the variation, and the statistics of the simulated values take precedence over the accuracy of the local estimates.

Stochastic simulation may still make use of the kriging equations. There are several methods; the one that we used for this analysis was sequential gaussian conditional simulation. In it the conditioning data for estimation include not only the original data but also all of the values that have been simulated previously within the given search neighbourhood. For this analysis we modified the programs in GSLIB (Deutsch & Journel, 1992)

The simulated values were conditioned on the data in the selected files in Table 8. In conditional gaussian simulation the conditional cumulative distribution function (ccdf) is assumed to be Gaussian and the means and variances are given by a series of simple kriging systems. The data were transformed first to a standard normal distribution using a normal scores transform. The variogram was then computed from the transformed values of the entire set of values of the subset, and modelled. The model was a nested spherical one with similar ranges to that computed from the untransformed data.

The variable was simulated at the unknown points sequentially using simple kriging where the mean is assumed to be known. Since the data were normal scores we could assume that the mean was zero. The conditioning data were the original data and the simulated data for the given neighbourhood. At each node a specific number of neighbouring conditioning data including any previously simulated values were used with the variogram model and simple kriging to estimate the mean

and variance of the ccdf there. The simulated value was then determined from that ccdf. The new simulated value was then added to the data set for the next estimate to be computed. This was repeated at each node of the grid. At those with the original data the procedure returned the original value. Finally the simulated values were back-transformed to the original values, the resulting estimates were mapped, Figures 13, 15, 17, 19, 21, and 23.

Results

Figures 12 to 23 show the maps of the reconstructed image data for Benncut. We started by reducing the data to 25 %. It is clear in Figure 12 where the data were reconstructed by kriging that there has been some smoothing of the variation. The road in the south west of the image, a dark linear structure in Figure 11, is no longer as clear in Figure 12. For the conditional simulation, Figure 13, there has been less smoothing, and the overall variation has been preserved. Visually this map appears to represent the image more precisely. The road in the south west of the image has been retained more effectively than by kriging. The estimates at the unsampled points were compared with the original values at these points: Table 9 gives the mean differences and mean squared difference between the original values and the estimated values by kriging and simulation. For both methods the mean difference is small, showing that there is little bias in the results. The mean squared difference is smaller for kriging than for simulation, showing that the kriged estimates are closer to the true values. This first stage of data reduction shows clearly the different underlying aims of the methods: kriging obtains the best local estimates, whereas simulation preserves the variability and the statistical parameters of the distribution. The mean of the original DNs for the red channel of Benncut is 26.2, and the variance is 2.6065. Table 9 shows that the variance for the kriged estimates is less than the original variance and that for the simulated values.

Table 9: Summaries of kriging (K) and simulation (S) errors for Benncut.

Sampling interval	Mean difference		Mean squared difference		Mean of estimates		Mean Variance of estimates	
	K	S	K	S	K	S	K	S
1 in 2×2	−0.0330	0.0003	0.6908	1.8838	26.196	26.226	1.7957	2.6425
1 in 3×3	−0.0222	−0.0085	1.0116	2.2883	26.195	26.218	1.5115	2.4156
1 in 4×4	0.0592	0.0589	1.1104	3.0634	26.276	26.281	1.5336	2.8254
1 in 5×5	−0.0142	0.0056	1.5265	3.1271	26.211	26.231	1.3469	2.5920
1 in 6×6	−0.0199	−0.0064	1.6837	3.6283	26.210	26.216	0.9253	2.5700
1 in 7×7	−0.1464	−0.0942	1.8512	4.2432	26.083	26.131	0.0503	3.1130

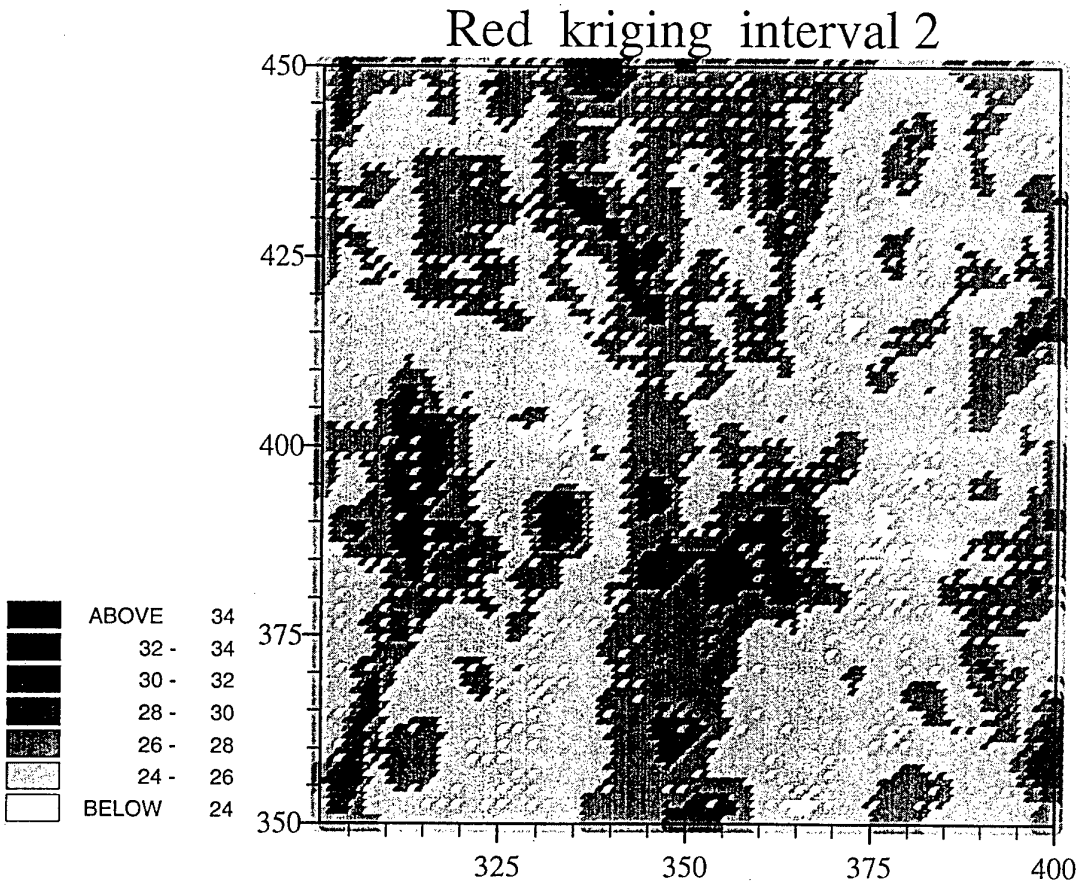

Figure 12: Map of ordinary kriged estimates for Benncut from a sample of 1 in 2 × 2 (25 %).

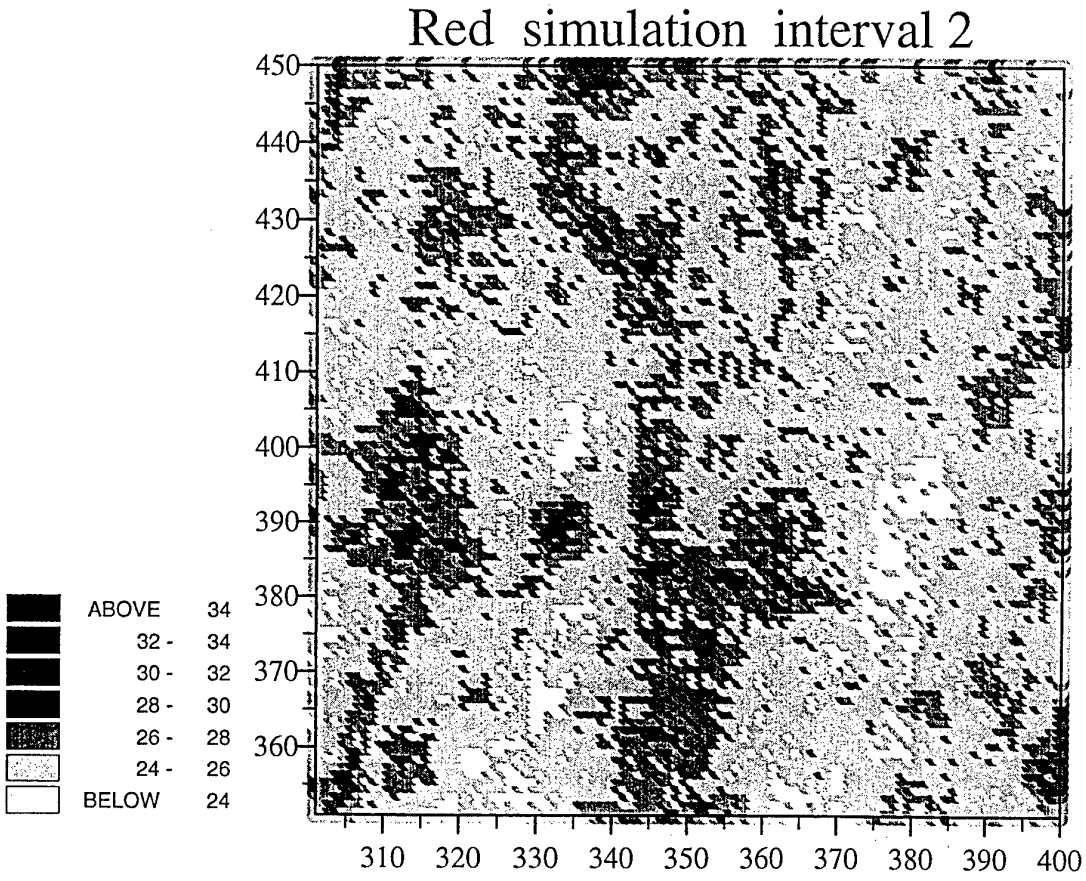

Figure 13: Map of estimates for Benncut by conditional Gaussian sequential simulation from a sample of 1 in 2 × 2 (25 %).

Figures 14 and 15 show the results for the 1 in 3 × 3 sample. In both cases the general forms of the main structures have been retained, but the effect of smoothing by kriging (Figure 14) is now more evident. The mean squared difference for simulation has increased more than that for kriging. For the 1 in 4 × 4 sampling the results of kriging, Figure 16, shows that the main structures are still evident, but the road in the south western part of the area is not. This structure can still be seen in the simulated map, Figure 17. In general the latter appears to be more similar to the original map than the kriged one. Figure 18 for kriging from the 1 in 5 × 5 sample shows that the major structures have been retained reasonably well, but that the fine detail has been lost. The map of the simulated values for this data set, Figure 19, shows that the variability in the original image has been retained as well as the form of the larger structures. Figure 20, kriging of 1 in 6 × 6 data, shows again that kriging has retained the main large scale structures in the centre of the field, but that the edges are now becoming less precise. The map of the simulated values, Figure 21 is more like the original map than the kriged one. Even for Figures 22 and 23, 1 in 7 × 7 data, there is reasonable reproduction of the general form of the large-scale features. It is unlikely that data would need to be compressed to this extent, but the results show clearly the capabilities of kriging and geostatistical simulation for restoring the information once a good spatial model has been derived.

The mean differences between the values for simulation remain small throughout, but the mean squared differences are slightly larger than for kriging. One factor that might have made the results of simulation appear less precise than the kriged ones is the effect of transformation. The back transformation results in some aberrant values from the tails of the distribution. Nevertheless considering that 75% and more of the data have been eliminated the results are good for both methods. It also confirms that there is considerable redundant information in remotely sensed data, as suggested by Atkinson *et al.* (1990). The results suggest that once we have a good variogram model it is possible to reconstruct the image reliably from a small sample. There is now a need to apply simulated annealing to this test because it does not depend on transformed values, so that we can explore further the results from simulation.

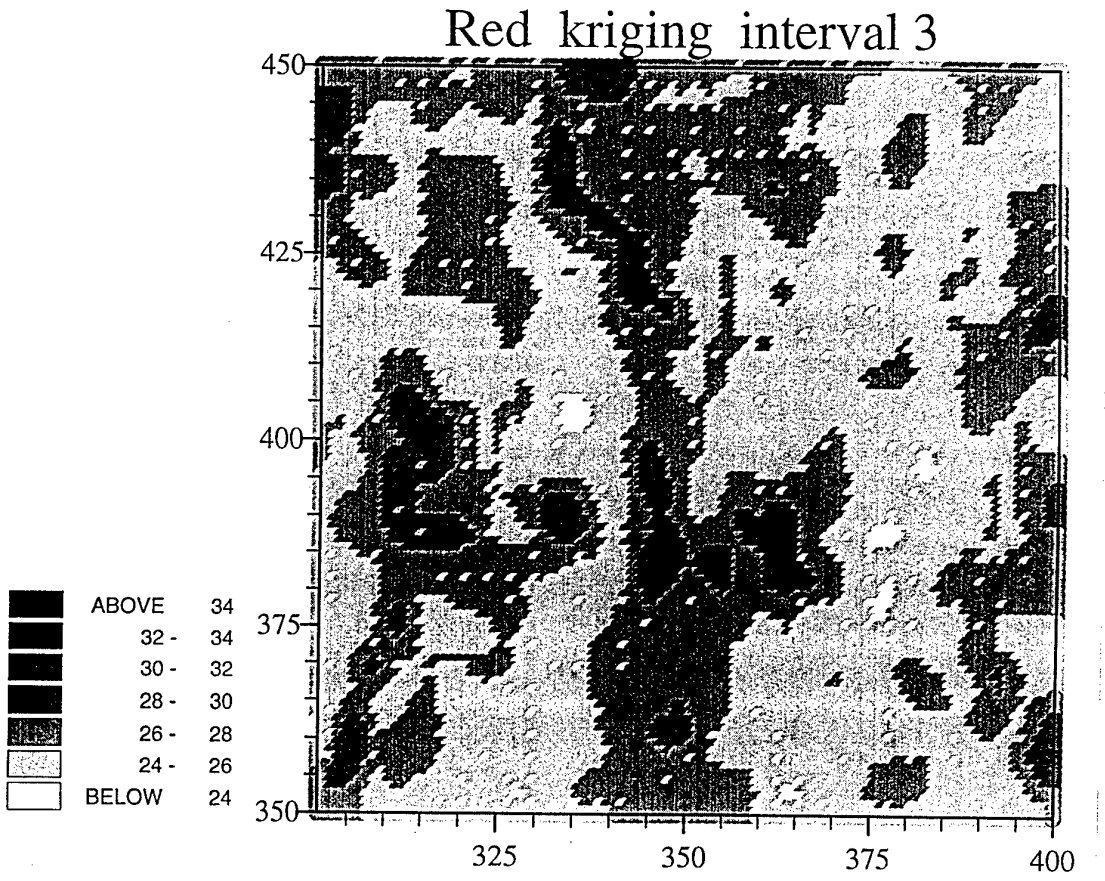

Figure 14: Map of ordinary kriged estimates for Benncut from a sample of 1 in 3 × 3 (11.22 %).

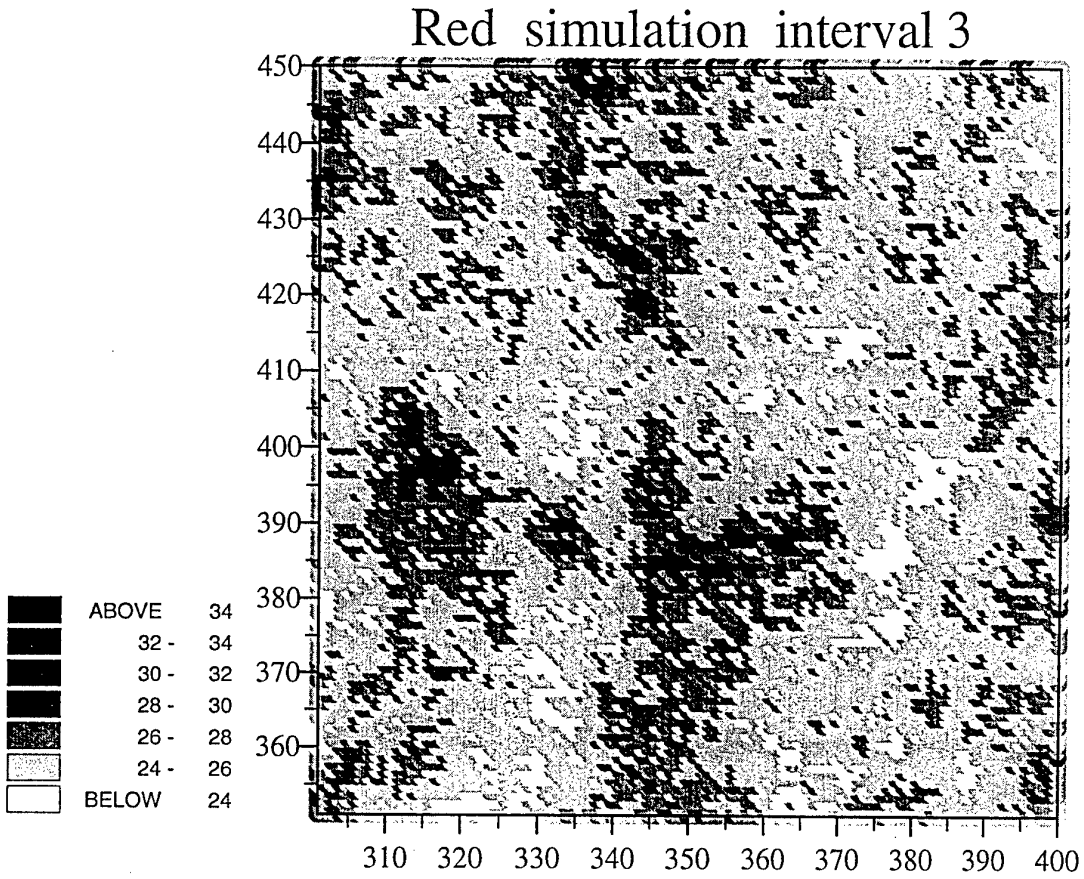

Figure 15: Map of estimates for Benncut by conditional Gaussian sequential simulation from a sample of 1 in 3 × 3 (11.22 %).

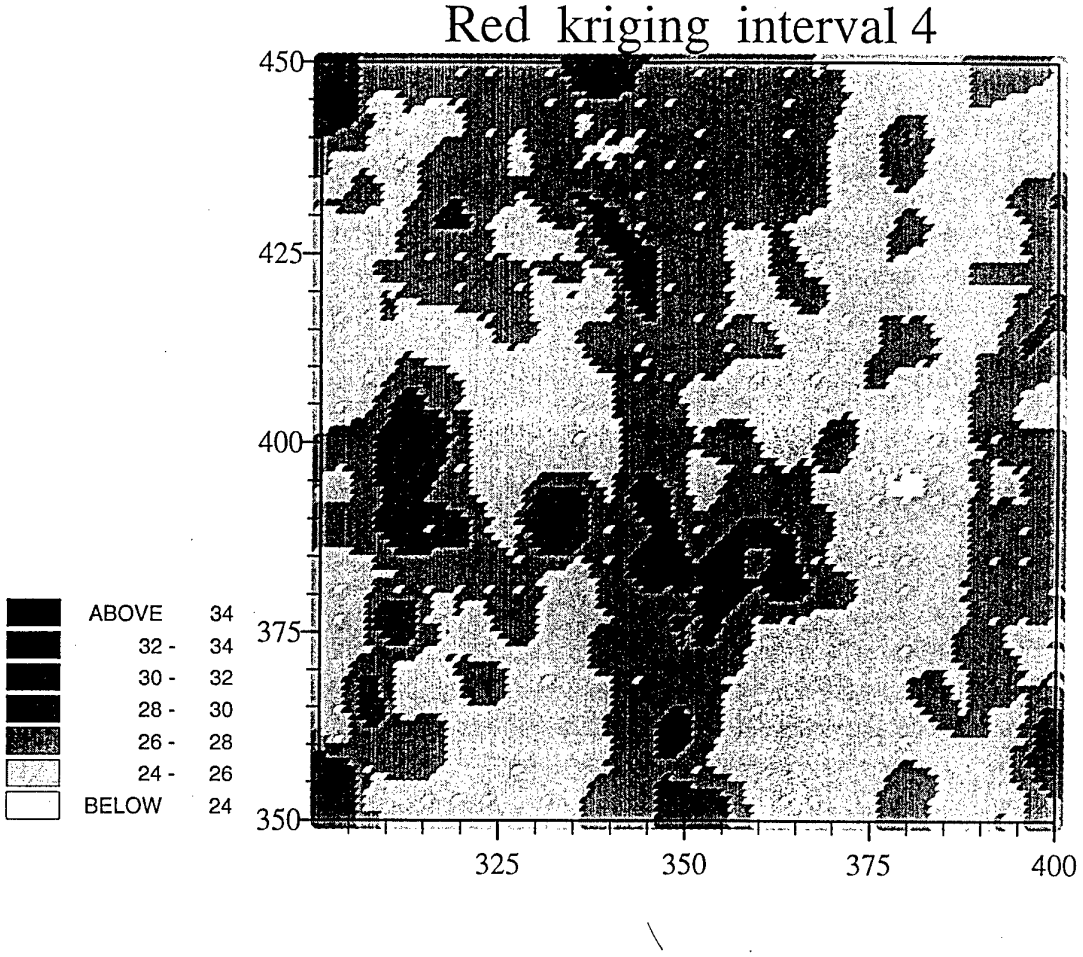

Figure 16: Map of ordinary kriged estimates for Benncut from a sample of 1 in 4 × 4 (6.25 %).

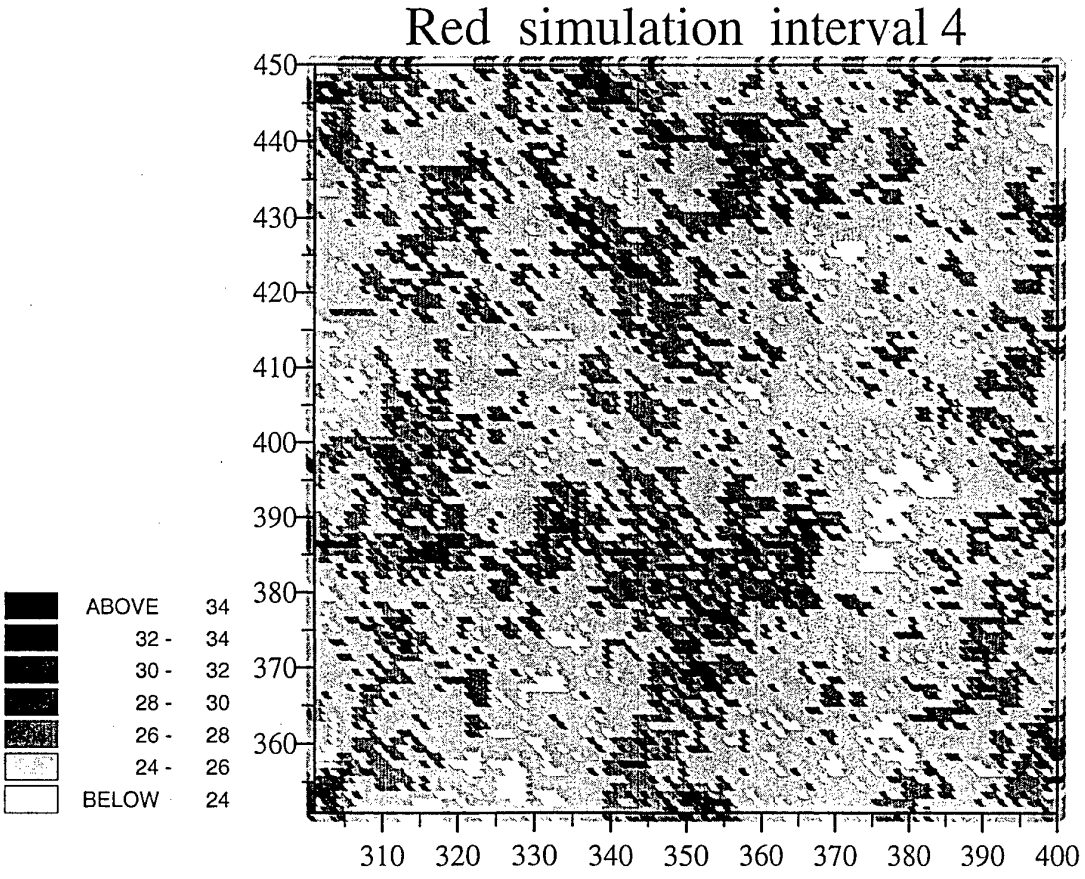

Figure 17: Map of estimates for Benncut by conditional Gaussian sequential simulation from a sample of 1 in 4 $\times$ 4 (6.24 %).

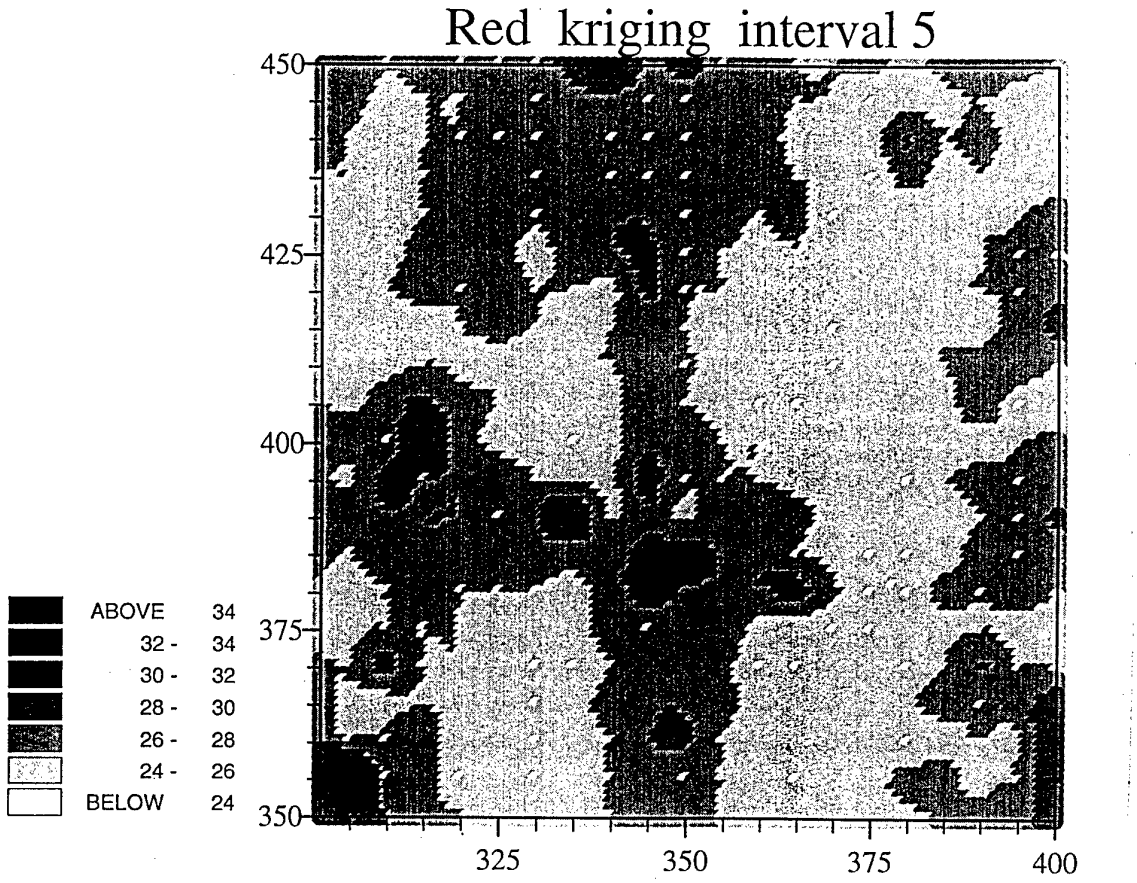

Figure 18: Map of ordinary kriged estimates for Benncut from a sample of 1 in 5 × 5 (4 %).

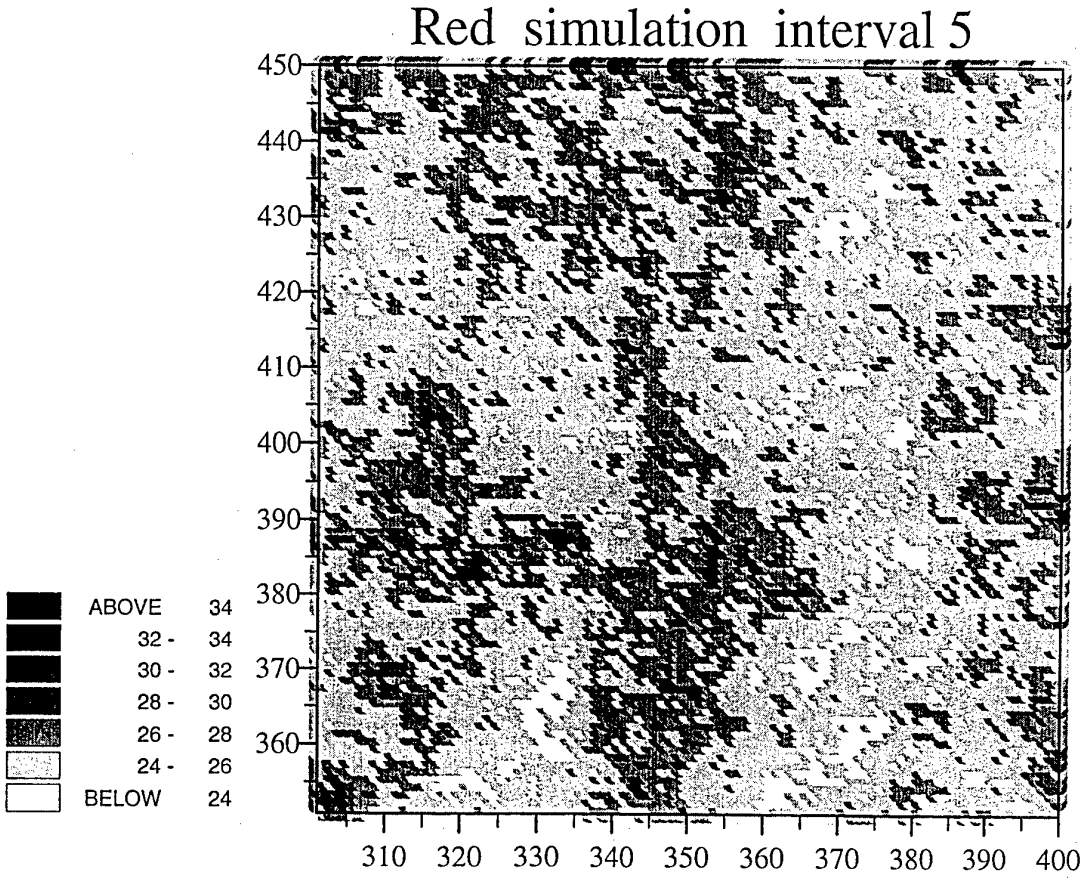

Figure 19: Map of estimates for Benncut by conditional Gaussian sequential simulation from a sample of 1 in 5 $\times$ 5 (4 %).

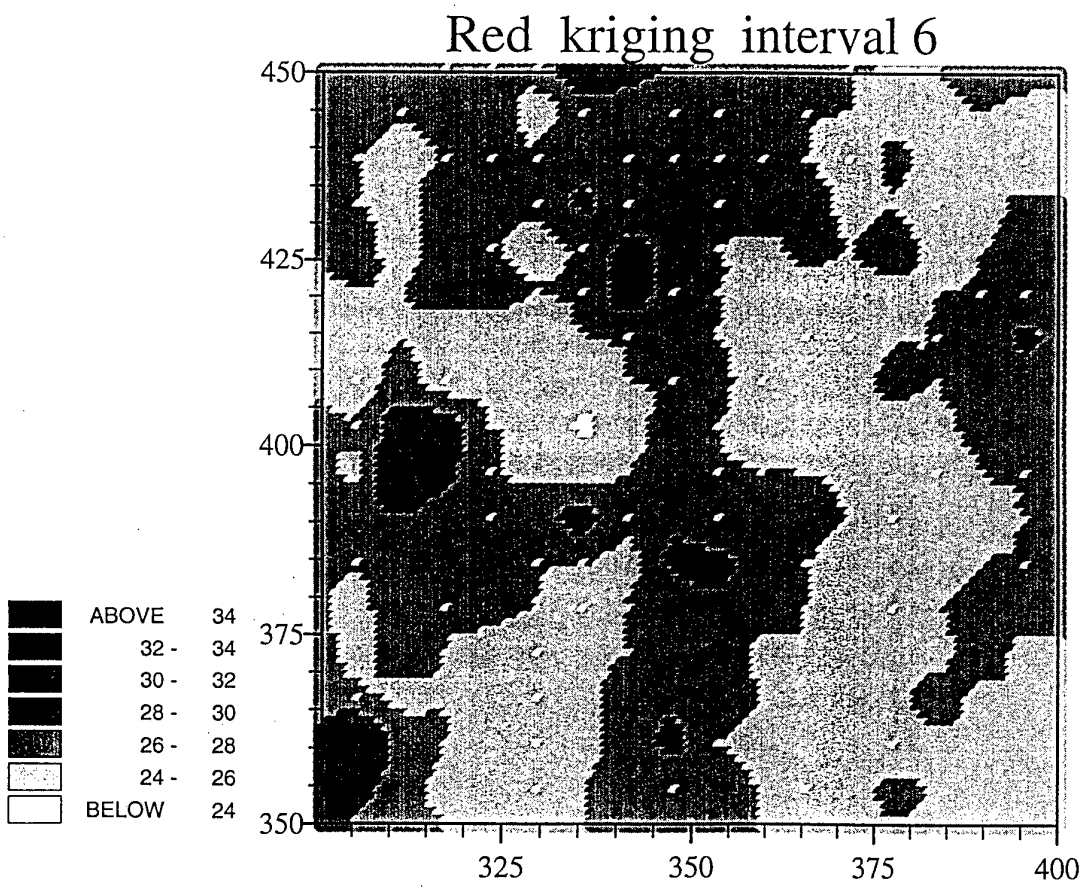

Figure 20: Map of ordinary kriged estimates for Benncut from a sample of 1 in 6 × 6 (2.72 %).

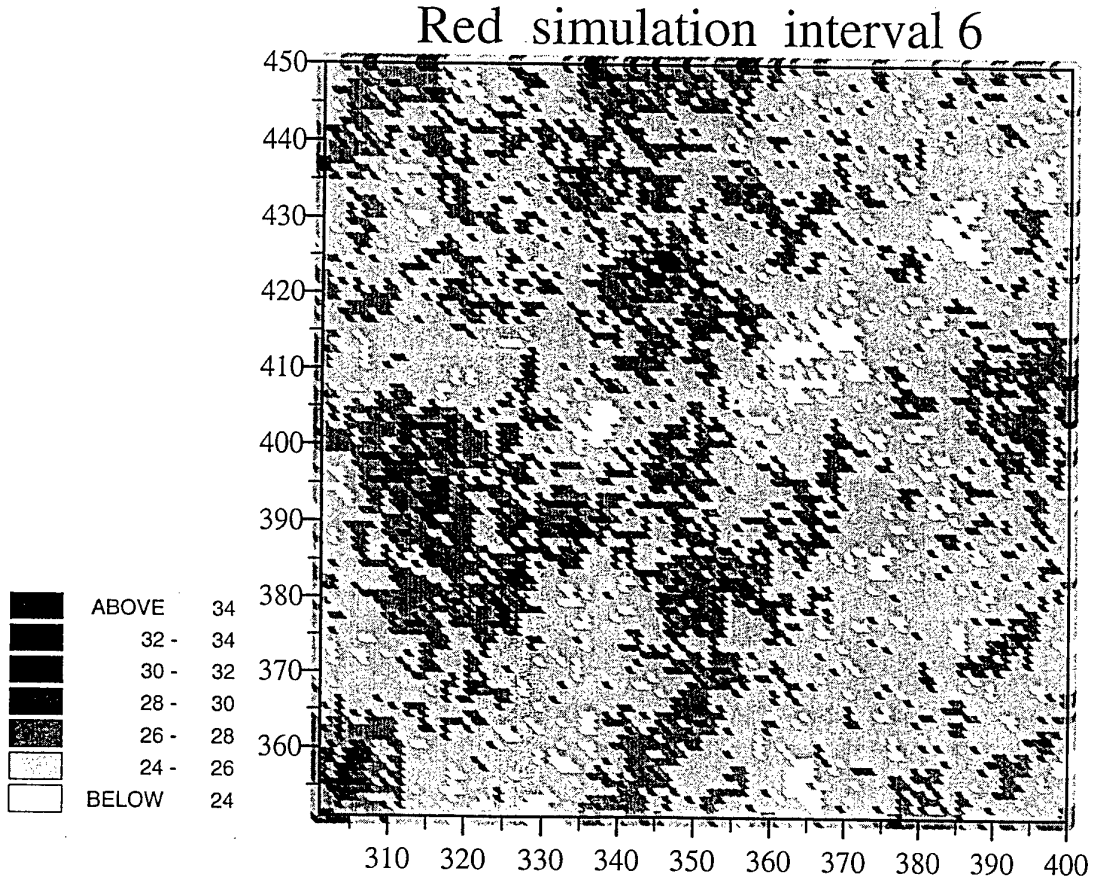

Figure 21: Map of estimates for Benncut by conditional Gaussian sequential simulation from a sample of 1 in 6 × 6 (2.72 %).

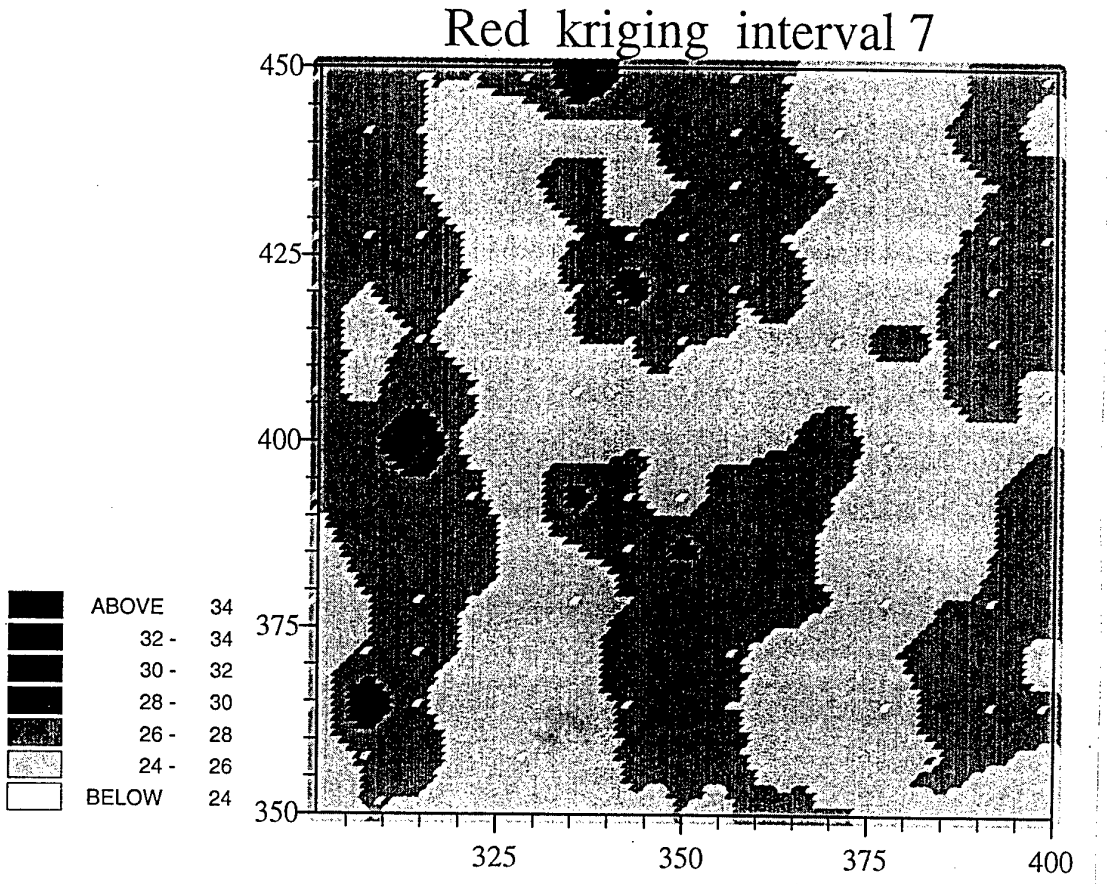

Figure 22: Map of ordinary kriged estimates for Benncut from a sample of 1 in 7 $\times$ 7 (2.1 %).

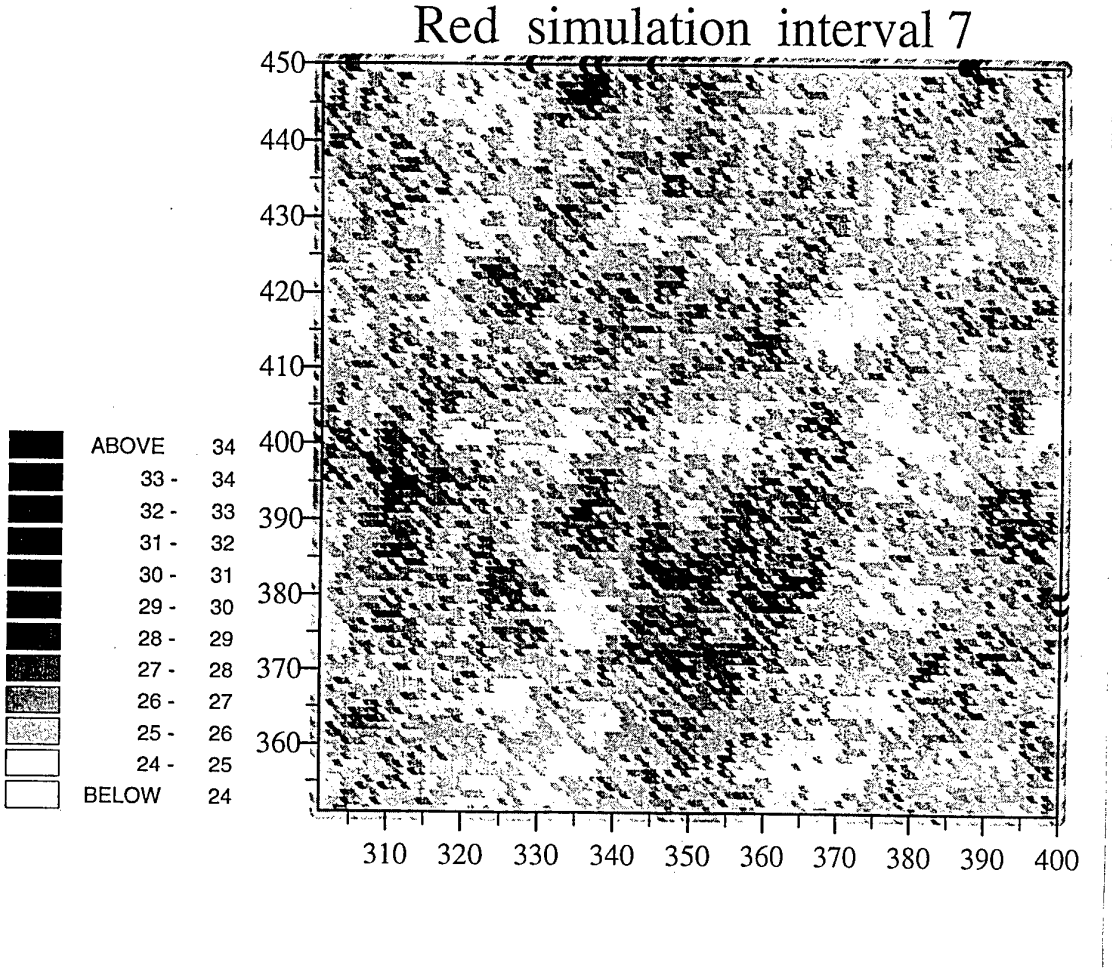

Figure 23: Map of estimates for Benncut by conditional Gaussian sequential simulation from a sample of 1 in 7 × 7 (2.1 %).

BIBLIOGRAPHY

Atkinson, P. Curran, P. J. & Webster , R. 1990 Sampling remotely sensed imagery for storage, retrieval and reconstruction. *Professional Geographer*, **42**, 345-353.

Bourgault, G. & Marcotte, D. 1993. Spatial filtering under the linear coregionalization model. In: A. Soares (ed.) *Geostatistics Troiá '92*, pp. 237-248.

Burgess, T. M. & Webster, R. 1980 Optimal interpolation and isarithmic mapping of soil properties. I. The semi-variogram and punctual kriging. *Journal of Soil Science,* 31, 315-331.

Deutsch, C. V. & Journel, A. J. 1996. *GSLIB Geostatistical Software Library and User's Guide*, Oxford University Press, New York.

Galli, A., Gerdil-Neuillet, F. & Dadou, C. 1984 Factorial kriging analysis: a substitute to spectral analysis of magnetic data. In: *Geostatistics for Natural Resource Characterization* (eds G. Verly *et al.*), pp 543-557. D. Reidel, Dordrecht.

Genstat 5 Committee 1987 *Genstat 5 Reference Manual.* Oxford University Press.

Goulard, M & Voltz, M. 1992 Linear coregionalization model: tools for estimation and choice of cross-variogram matrix. *Mathematical Geology*, **24**, 269-286.

Goovaerts, P. & Webster. R. 1994. Scale-dependent correlation between topsoil copper and cobalt concentrations in Scotland. *European Journal of Soil Science*, **45**, 79-95.

Jaquet, O. 1989 Factorial kriging analysis applied to geological data from petroleum exploration. *Mathematical Geology*, **21**, 683-691.

Journel, A. G. & Huijbregts, C. J. 1978 *Mining Geostatistics.* Academic Press, London.

Matheron, G. 1982 *Pour une analyse krigeante de données régionalisées.* Note N-732, Centre de Géostatistique, Ecole des Mines de Paris, Fontainebleau.

Whittle, P. 1954. On stationary processes in the plane. *Biometrika*, 41, 434-449.

Ross, G. J. S. 1987 *MLP Maximum Likelihood Program.* Numerical Algorithms Group, Oxford.

Wackernagel, H. 1994. Cokriging versus kriging in regionalized multivariate data analysis, *Geoderma*, **62**, 83-92.

Webster, R. & Oliver, M. A. 1990 *Statistical Methods in Soil and Land Resource Survey.* Oxford University Press.

Wen, R. & Sinding-Larsen, R. 1997. Geostatistics for image analysis. In: E. Baafi (ed.), *Proceedings of the Fifth International Geostatistics Congress, Wollongong*, (in press).

APPENDIX 1 Genstat Directives

The FVARIOGRAM directive

The FVARIOGRAM directive forms an experimental variogram from a set of values of a variable, Z, distributed in one or two dimensions using the usual computing formula:

$$\hat{\gamma}(\mathbf{h}) \quad = \quad \frac{1}{2m(\mathbf{h})} \sum_{i=1}^{m(\mathbf{h})} \{z(\mathbf{x}_i) - z(\mathbf{x}_i + \mathbf{h})\}^2 \ , \tag{21}$$

where $z(\mathbf{x}_i)$ and $z(\mathbf{x}_i + \mathbf{h})$ are the values at positions $\mathbf{x}_i$ and $\mathbf{x}_i + \mathbf{h}$, and $m(\mathbf{h})$ is the number of paired comparisons contributing to the estimate. For data on a regular grid or transect $\mathbf{h}$ is an integer multiple of the sampling interval. For irregularly scattered data $\mathbf{h}$ is discretized so that for each nominal lag there is a range of distance equal to the increment (STEP) and an angular range (SEGMENTS) set by the user. The nominal lag is at the centre of both ranges.

Data (DATA) may be on a regular grid and read as a matrix with coordinates implied by columns (X) and rows (Y). Alternatively they may be irregularly scattered, in which case they are read as a variate, and they must have their spatial coordinates provided as X (eastings) and Y (northings), also in variates.

The experimental variogram is controlled by five options. For irregular data the maximum distance to which the variogram is calculated is set by XMAX for all directions. For regular data XMAX defines the maximum lag distance in the X direction, and additionally YMAX must be given to limit the distance in the Y direction. The increment in distance is set by STEP. The variogram may be computed in one or more directions. These are given by DIRECTIONS in degrees counterclockwise from east in the usual mathematical convention. Each direction is at the centre of an angular range, which is defined by SEGMENTS.

A variogram can be computed without regard to direction by setting DIRECTIONS to 0 and SEGMENTS to 180. This is advisable if variation seems to be isotropic, i.e. the same in all directions, or if there are too few data to compute $\hat{\gamma}(\mathbf{h})$ for two or more directions separately. The lag then becomes a scalar $|\mathbf{h}| = h$ in distance only. Experience suggests that some 300 data are needed to distinguish anisotropy.

Statistics are provided by default, and the user can obtain one or more graphs of the variogram by setting GRAPH in the PRINT option.

The final output of FVARIOGRAM is a set of variates as follows.

VARIOGRAMS – the ordered set of semivariances.

DISTANCES – the mean lag distances at which the semivariances have been computed.

DIRECTIONS – the angular separations at which the semivariances have been calculated.

COUNTS – the numbers of paired comparisons from which the semivariances have been computed.

These are tabulated on output in columns in the order DISTANCES, ANGLES, VARIOGRAMS, and COUNTS, from which they can be read for the next stage of analysis, the fitting of models using MVARIOGRAM.

The MVARIOGRAM procedure

The procedure MVARIOGRAM fits one or more models to the experimental variogram. It uses the Genstat directive FITNONLINEAR. Models must be authorized in the sense that they cannot give rise to negative variances when data are combined. Technically they are conditionally negative semi-definite (CNSD); see Webster & Oliver (1990) or Journel & Huijbregts (1978) for an explanation.

The isotropic models currently available in MVARIOGRAM are:

bounded with finite range – BOUNDEDLINEAR (bounded linear) , CIRCULAR, SPHERICAL, DOUBLESPHERICAL (double spherical) and PENTASPHERICAL;

bounded asymptotic – EXPONENTIAL, BESSELK1 (Whittle's elementary correlation; Whittle, 1954), and GAUSSIAN.

unbounded – POWERFUNCTION (power function with exponent strictly between 0 and 2), and LINEAR, which is a special case of the power function with exponent 1.

In addition the AFFINEPOWER function may be fitted to an experimental variogram that appears unbounded and geometrically anisotropic, i.e. one that might be made isotropic by a simple linear transformation of the spatial coordinates.

The procedure takes a table of DISTANCES, ANGLES, VARIOGRAMS, and COUNTS, as produced by FVARIOGRAM, and it attempts to fit in turn the models specified by the user by estimating their parameters. It weights the entries in the experimental variogram, either by the COUNTS, or by a combination of COUNTS and VARIOGRAM using the setting CBYVAR, or equally using the setting EQUAL. The model may be fitted with an intercept (a constant, the 'nugget' variance, see below) by setting ESTIMATE, or through the origin with the setting OMIT.

Output from the procedure includes convergence monitoring, an analysis of variance, and the estimated values of the parameters, distinguishing the non-linear from the linear.

The procedure contains or calculates from the variogram rough starting values for the parameters. These are then refined by FITNONLINEAR to convergence. If the solution does not converge there are two likely reasons.

1. The model is unsuited for the particular experimental variogram. For example, a bounded model is specified when the variogram is clearly unbounded, or *vice versa*. The user should choose only variograms that have approximately the right shape.
2. The starting values are too far from a sensible solution. Here the user should estimate starting values by inspection and insert them into MVARIOGRAM.

The KRIGE directive

The KRIGE directive computes the ordinary kriging estimates of a variable at positions on a grid from data and a model variogram by solving the kriging system.

The DATA must be in one of the two forms as for FVARIOGRAM, i.e. as a matrix on a rectangular grid with spatial coordinates implied, or as a variate with the coordinates in X (eastings) and Y (northings) supplied as additional variates. By default all data are considered when forming the kriging system. However, a subset of the data may be selected by limiting the area to a rectangle defined by XOUTER, the left (western) and right (eastern) limits, and YOUTER, the bottom (southern) and top (northern) limits.

The positions at which Z is estimated (predicted) are contained in a rectangle defined by XINNER and YINNER and INTERVAL. XINNER and YINNER are specified in the same way as XOUTER and YOUTER, and their limits should lie within those of XOUTER and YOUTER. The option INTERVAL is the distance between successive positions in the rows and columns of the grid at which kriging is to be done. INTERVAL is specified in the same units as the data. However, if the aim is to make a map then INTERVAL should be chosen so that it is no more than 2 mm on the final document. By doing this the optimality of kriging will not be noticeably degraded by the subsequent contouring.

Kriging may be either punctual, i.e. at 'points' which have the same size and shape as the sample support, or on bigger rectangular blocks. The size of the blocks is specified by BLOCK, the lengths of the block in the x direction (eastings) and y direction (northings). Punctual kriging is the default. Alternatively it can be specified by giving both values as 0. The average semivariances between point and block, $\bar{\gamma}(\mathbf{h})$ and $\bar{\gamma}(B,B)$ in the kriging system, are computed by integrating the variogram numerically over the block. The number of steps in each direction is given by NSTEP. The default is 8, and is recommended. The kriging may be accelerated by reducing NSTEP at the expense of accuracy, and accuracy gained by increasing it but by taking more time. The minimum is 4 and the maximum 10.

The minimum and maximum number of points for the kriging system, n in kriging equations, are set by MINPTS and MAXPTS. Their limits are a minimum of 3 for MINPTS and and maximum of 40 for MAXPTS, and MINPTS must be less than

or equal to MAXPTS. The defaults are 7 and 20 respectively. Data points may be selected around the point or block to be kriged by setting a RADIUS within which they must lie. If the variogram is anisotropic then the SEARCH may also be ANISOTROPIC. The default is ISOTROPIC.

Further options are available for gridded data. Universal kriging may be invoked by setting the DRIFT to LINEAR or to QUADRATIC, i.e. of order 1 or 2 respectively. The default is CONSTANT for ordinary kriging. If the grid is not square then the ratio of the spacing in the y direction to that in the x direction is given by YXRATIO. The default is 1.0 for square. Missing data on the grid may be interpolated by punctual kriging as a preliminary by setting INTERPOLATE to YES. The default is NO.

The variogram is specified by its type and parameters, as follows. The MODEL may be of any of POWER, BOUNDEDLINEAR (one dimension only), CIRCULAR, SPHERICAL, PENTASPHERICAL, DOUBLESPHERICAL, EXPONENTIAL, GAUSSIAN, and BESSELK1 (Whittle's function). All models may have a NUGGET, which is the constant from MVARIOGRAM. The POWER function (the only unbounded model) has a GRADIENT and EXPONENT. The simple bounded models, i.e. all others except DOUBLESPHERICAL, have SILLVARIANCES (the sill of the correlated variance) and RANGES. The latter is strictly the correlation range of the BOUNDEDLINEAR, CIRCULAR, SPHERICAL AND PENTASPHERICAL models, and for the asymptotic ones it is the distance parameter of the model. The DOUBLESPHERICAL model has two SILLVARIANCES and two RANGES corresponding to the two components of the model.

The ISOTROPY may be ISOTROPIC or anisotropic. In the latter case it may be either BURGESS anisotropy (Burgess & Webster, 1980) or GEOMETRIC anisotropy (Journel & Huijbregts, 1978; Webster & Oliver, 1990), and the anisotropy must be specified by three parameters, namely PHI, the angle in radians of the direction of maximum variation, RMAX, the maximum gradient of the model, and RMIN, the minimum gradient. In the present release only the POWER function may be anisotropic.

The output consists of two matrices, one of estimates (predictions) in ESTIMATES, and the other of the estimation (prediction or kriging) variances in VARIANCES. The matrices are arranged with the first row of each matrix at the bottom following geographic rather than mathematical convention, ready for mapping.

Intermediate results may be printed optionally by settings of PRINT. SEARCH will list the results of the search for data around each position to be kriged. WEIGHTS will list the kriging weights at each position. MONITOR will monitor the formation and inversion of the kriging matrices for each position. These options enable the user to check that the kriging is working reasonably. They can produce a great deal of output, and they should not be requested when kriging large matrices, such as might

be wanted for mapping. The option DATA will print the data.

APPENDIX 2 Results of Climate Data Analysis

Potential Evapotranspiration

X	Y	ESTIMATE	VARIANCE	ESTIMATE	VARIANCE	ESTIMATE	VARIANCE	PE
		Autokriging	121 points	Cokriging	121 points	Cokriging	121+56 points	Original
35.33	94.37	6.94E+01	8.04E+01	7.53E+01	6.78E+01	7.50E+01	6.44E+01	7.47E+01
34.73	92.23	4.97E+01	8.19E+01	8.60E+01	7.83E+01	8.50E+01	7.62E+01	9.58E+01
41.93	72.68	2.03E+01	7.42E+01	1.05E+02	4.43E+01	1.05E+02	3.84E+01	1.21E+02
38.85	77.03	2.97E+01	7.10E+01	8.59E+01	2.28E+01	8.13E+01	1.30E+01	7.74E+01
39.67	75.6	2.38E+01	7.01E+01	9.46E+01	2.65E+01	9.26E+01	1.77E+01	9.32E+01
30.22	81.88	9.20E+00	7.14E+01	6.95E+01	2.01E+01	6.90E+01	9.61E+00	7.31E+01
24.58	81.68	9.80E-01	8.27E+01	5.05E+01	1.67E+01	4.83E+01	3.29E+00	4.75E+01
32.52	84.95	4.54E+01	7.37E+01	8.90E+01	4.40E+01	8.94E+01	3.81E+01	8.53E+01
32.13	81.2	1.97E+01	7.27E+01	7.73E+01	3.34E+01	7.54E+01	2.56E+01	7.40E+01
41.98	87.9	7.26E+01	7.49E+01	8.91E+01	4.85E+01	8.91E+01	4.20E+01	8.29E+01
41.53	93.65	9.98E+01	7.81E+01	7.06E+01	6.29E+01	7.07E+01	5.94E+01	6.60E+01
42.08	87.83	7.28E+01	7.49E+01	8.89E+01	4.86E+01	8.87E+01	4.21E+01	8.33E+01
41.45	90.5	8.01E+01	7.72E+01	7.87E+01	5.75E+01	7.77E+01	5.31E+01	8.28E+01
40.67	89.68	7.21E+01	7.59E+01	8.08E+01	4.14E+01	8.05E+01	3.46E+01	8.01E+01
41	85.2	7.48E+01	7.30E+01	9.12E+01	4.36E+01	9.16E+01	3.77E+01	9.01E+01
38.03	84.6	8.63E+01	7.42E+01	9.43E+01	4.40E+01	9.52E+01	3.80E+01	1.01E+02
29.98	90.25	7.42E+00	7.45E+01	9.54E+01	2.24E+01	9.35E+01	1.19E+01	9.34E+01
38.28	76.42	1.93E+01	7.18E+01	8.59E+01	3.68E+01	8.33E+01	2.98E+01	8.35E+01
45.07	83.57	6.84E+01	8.43E+01	9.29E+01	7.16E+01	9.34E+01	6.84E+01	7.83E+01
42.97	83.75	7.23E+01	7.57E+01	8.54E+01	4.48E+01	8.52E+01	3.86E+01	7.58E+01
42.77	84.6	7.24E+01	7.44E+01	8.67E+01	4.10E+01	8.73E+01	3.42E+01	7.82E+01
46.83	92.18	1.10E+02	8.99E+01	6.11E+01	8.93E+01	6.15E+01	8.72E+01	7.80E+01
44.88	93.22	1.12E+02	8.28E+01	6.00E+01	6.42E+01	5.85E+01	6.00E+01	5.93E+01
38.82	92.22	8.08E+01	7.92E+01	7.84E+01	6.49E+01	7.86E+01	6.14E+01	8.54E+01
32.32	90.08	2.50E+01	7.72E+01	9.59E+01	6.04E+01	9.69E+01	5.66E+01	9.88E+01
32.33	88.75	2.58E+01	7.37E+01	9.96E+01	2.38E+01	1.01E+02	1.38E+01	9.70E+01
35.27	75.55	2.62E+00	8.53E+01	8.83E+01	8.08E+01	8.71E+01	7.84E+01	1.00E+02
35.22	80.93	7.40E+01	7.24E+01	8.47E+01	4.22E+01	8.59E+01	3.62E+01	8.01E+01
34.9	76.88	7.29E+00	7.74E+01	8.88E+01	3.77E+01	8.79E+01	2.98E+01	8.96E+01
46.9	96.8	1.44E+02	9.34E+01	4.81E+01	1.19E+02	4.79E+01	1.19E+02	4.10E+01
42.87	100.55	2.43E+02	8.11E+01	3.63E+01	7.40E+01	3.67E+01	7.14E+01	3.38E+01
39.45	74.57	1.64E+01	7.29E+01	9.81E+01	3.40E+01	9.80E+01	2.63E+01	9.56E+01
42.22	75.98	4.37E+01	7.19E+01	9.51E+01	3.44E+01	1.02E+02	2.70E+01	1.02E+02
40.65	73.78	1.90E+01	7.22E+01	1.02E+02	1.88E+01	9.84E+01	7.95E+00	9.49E+01
40.92	81.43	8.21E+01	7.33E+01	9.36E+01	3.19E+01	9.63E+01	2.38E+01	9.31E+01
35.4	97.6	1.36E+02	8.06E+01	5.08E+01	7.25E+01	5.14E+01	6.94E+01	5.41E+01
42.83	80.18	6.96E+01	7.63E+01	9.54E+01	4.49E+01	9.64E+01	3.88E+01	1.06E+02
40.5	80.22	7.74E+01	7.54E+01	9.49E+01	4.70E+01	9.70E+01	4.16E+01	9.22E+01
35.03	85.2	7.56E+01	7.57E+01	9.91E+01	5.68E+01	9.96E+01	5.25E+01	1.09E+02
35.8	84	9.41E+01	7.52E+01	9.25E+01	5.84E+01	9.32E+01	5.45E+01	9.60E+01
36.12	86.68	6.35E+01	7.74E+01	1.05E+02	5.85E+01	1.06E+02	5.44E+01	9.69E+01
32.42	99.68	1.67E+02	7.95E+01	3.06E+01	6.15E+01	3.18E+01	5.73E+01	3.33E+01
35.23	101.7	2.72E+02	8.55E+01	2.46E+01	7.64E+01	2.64E+01	7.36E+01	2.94E+01
25.9	97.43	2.65E+01	9.66E+01	4.01E+01	1.16E+02	3.89E+01	1.15E+02	3.14E+01
27.7	97.28	2.36E+01	7.53E+01	4.25E+01	2.25E+01	3.92E+01	1.17E+01	3.64E+01
32.9	97.03	8.45E+01	7.62E+01	5.14E+01	2.02E+01	5.03E+01	8.99E+00	4.92E+01
29.97	95.35	2.06E+01	7.71E+01	6.89E+01	5.43E+01	6.84E+01	4.96E+01	6.95E+01
29.53	98.47	7.49E+01	7.81E+01	3.47E+01	6.12E+01	3.54E+01	5.72E+01	4.00E+01
33.97	98.48	1.47E+02	8.14E+01	4.17E+01	7.95E+01	4.05E+01	7.69E+01	4.21E+01
36.93	76.28	1.14E+01	7.20E+01	8.53E+01	1.54E+01	8.26E+01	3.59E+00	7.10E+01
38.95	77.45	3.69E+01	7.18E+01	8.60E+01	2.85E+01	8.15E+01	1.99E+01	8.90E+01
42.95	87.9	7.47E+01	7.50E+01	8.28E+01	4.69E+01	8.24E+01	4.08E+01	8.04E+01
37.78	81.12	9.39E+01	7.32E+01	8.59E+01	3.58E+01	9.30E+01	2.84E+01	9.64E+01
44.88	63.52	1.82E+01	8.05E+01	1.79E+02	2.43E+01	1.84E+02	1.32E+01	1.88E+02
46.8	71.38	2.54E+01	9.60E+01	1.44E+02	1.34E+02	1.44E+02	1.34E+02	1.25E+02
43.9	69.93	1.78E+01	7.82E+01	1.44E+02	3.39E+01	1.43E+02	2.54E+01	1.42E+02

Continentality

X	Y	ESTIMATE	VARIANCE	ESTIMATE	VARIANCE	ESTIMATE	VARIANCE	Continentality
		Autokriging	121 points	Cokriging	121 points	Cokriging	121+56 points	Original
35.33	94.37	4.33E+01	1.16E+01	4.35E+01	1.12E+01	4.37E+01	1.10E+01	4.44E+01
34.73	92.23	3.85E+01	1.25E+01	3.89E+01	1.20E+01	3.90E+01	1.20E+01	4.24E+01
41.93	72.68	4.21E+01	9.33E+00	4.18E+01	9.07E+00	4.17E+01	8.71E+00	4.36E+01
38.85	77.03	3.97E+01	8.06E+00	3.89E+01	7.73E+00	3.99E+01	7.10E+00	3.99E+01
39.67	75.6	4.07E+01	7.98E+00	4.00E+01	7.77E+00	4.08E+01	7.18E+00	4.05E+01
30.22	81.88	2.64E+01	7.97E+00	2.55E+01	7.61E+00	2.56E+01	6.96E+00	2.70E+01
24.58	81.68	1.11E+01	9.69E+00	1.20E+01	8.83E+00	1.15E+01	8.26E+00	9.30E+00
32.52	84.95	3.57E+01	9.29E+00	3.59E+01	9.00E+00	3.57E+01	8.66E+00	3.49E+01
32.13	81.2	3.16E+01	8.76E+00	3.04E+01	8.45E+00	3.09E+01	8.00E+00	3.25E+01
41.98	87.9	4.77E+01	9.67E+00	4.75E+01	9.39E+00	4.76E+01	8.93E+00	4.83E+01
41.53	93.65	5.38E+01	1.10E+01	5.33E+01	1.06E+01	5.36E+01	1.05E+01	5.35E+01
42.08	87.83	4.75E+01	9.64E+00	4.74E+01	9.36E+00	4.75E+01	8.90E+00	4.71E+01
41.45	90.5	5.12E+01	1.04E+01	5.08E+01	1.01E+01	5.13E+01	9.88E+00	5.12E+01
40.67	89.68	4.98E+01	9.66E+00	4.93E+01	9.23E+00	4.95E+01	8.88E+00	4.95E+01
41	85.2	4.49E+01	9.13E+00	4.50E+01	8.89E+00	4.51E+01	8.54E+00	4.68E+01
38.03	84.6	4.23E+01	9.46E+00	4.20E+01	9.15E+00	4.17E+01	8.83E+00	4.19E+01
29.98	90.25	3.02E+01	8.57E+00	2.95E+01	8.09E+00	3.00E+01	7.52E+00	2.86E+01
38.28	76.42	3.87E+01	8.55E+00	3.76E+01	8.32E+00	3.83E+01	7.87E+00	3.91E+01
45.07	83.57	4.33E+01	1.22E+01	4.31E+01	1.16E+01	4.31E+01	1.16E+01	4.24E+01
42.97	83.75	4.39E+01	9.74E+00	4.36E+01	9.38E+00	4.36E+01	9.02E+00	4.40E+01
42.77	84.6	4.40E+01	9.24E+00	4.39E+01	8.93E+00	4.36E+01	8.51E+00	4.41E+01
46.83	92.18	5.52E+01	1.38E+01	5.50E+01	1.33E+01	5.52E+01	1.32E+01	5.14E+01
44.88	93.22	5.58E+01	1.18E+01	5.57E+01	1.13E+01	5.63E+01	1.11E+01	5.76E+01
38.82	92.22	4.82E+01	1.12E+01	4.83E+01	1.08E+01	4.85E+01	1.07E+01	4.87E+01
32.32	90.08	3.43E+01	1.07E+01	3.43E+01	1.04E+01	3.41E+01	1.02E+01	3.79E+01
32.33	88.75	3.55E+01	8.86E+00	3.59E+01	8.37E+00	3.57E+01	7.87E+00	3.51E+01
35.27	75.55	3.44E+01	1.32E+01	3.27E+01	1.26E+01	3.33E+01	1.26E+01	3.12E+01
35.22	80.93	3.66E+01	9.02E+00	3.76E+01	8.79E+00	3.71E+01	8.42E+00	3.66E+01
34.9	76.88	3.42E+01	9.67E+00	3.31E+01	9.19E+00	3.36E+01	8.75E+00	3.28E+01
46.9	96.8	5.71E+01	1.63E+01	5.63E+01	1.58E+01	5.62E+01	1.58E+01	5.93E+01
42.87	100.55	5.05E+01	1.20E+01	5.14E+01	1.16E+01	5.13E+01	1.16E+01	5.12E+01
39.45	74.57	3.98E+01	8.84E+00	3.89E+01	8.53E+00	3.88E+01	8.10E+00	4.07E+01
42.22	75.98	4.28E+01	8.66E+00	4.38E+01	8.37E+00	4.18E+01	7.91E+00	4.22E+01
40.65	73.78	4.09E+01	8.33E+00	3.99E+01	7.91E+00	4.05E+01	7.34E+00	3.97E+01
40.92	81.43	4.20E+01	8.76E+00	4.25E+01	8.37E+00	4.17E+01	7.89E+00	4.20E+01
35.4	97.6	4.70E+01	1.18E+01	4.67E+01	1.14E+01	4.66E+01	1.13E+01	4.70E+01
42.83	80.18	4.26E+01	9.67E+00	4.30E+01	9.28E+00	4.25E+01	8.96E+00	3.99E+01
40.5	80.22	4.08E+01	1.00E+01	4.14E+01	9.63E+00	4.13E+01	9.41E+00	4.11E+01
35.03	85.2	3.93E+01	1.03E+01	4.03E+01	1.00E+01	4.01E+01	9.79E+00	3.94E+01
35.8	84	3.83E+01	1.03E+01	3.98E+01	1.00E+01	3.92E+01	9.82E+00	3.87E+01
36.12	86.68	4.17E+01	1.07E+01	4.14E+01	1.04E+01	4.13E+01	1.02E+01	4.10E+01
32.42	99.68	4.23E+01	1.10E+01	4.36E+01	1.06E+01	4.31E+01	1.04E+01	4.20E+01
35.23	101.7	4.44E+01	1.28E+01	4.68E+01	1.23E+01	4.60E+01	1.23E+01	4.32E+01
25.9	97.43	2.78E+01	1.74E+01	2.66E+01	1.66E+01	2.66E+01	1.65E+01	2.63E+01
27.7	97.28	3.06E+01	8.34E+00	2.95E+01	8.00E+00	3.02E+01	7.29E+00	2.92E+01
32.9	97.03	4.31E+01	9.10E+00	4.26E+01	8.45E+00	4.31E+01	7.96E+00	4.29E+01
29.97	95.35	3.42E+01	1.03E+01	3.30E+01	1.00E+01	3.36E+01	9.80E+00	3.31E+01
29.53	98.47	3.60E+01	1.07E+01	3.61E+01	1.05E+01	3.59E+01	1.03E+01	3.64E+01
33.97	98.48	4.51E+01	1.23E+01	4.54E+01	1.20E+01	4.55E+01	1.18E+01	4.59E+01
36.93	76.28	3.64E+01	7.88E+00	3.52E+01	7.47E+00	3.64E+01	6.77E+00	3.64E+01
38.95	77.45	3.98E+01	8.48E+00	3.89E+01	8.14E+00	4.00E+01	7.61E+00	4.24E+01
42.95	87.9	4.78E+01	9.42E+00	4.76E+01	9.15E+00	4.76E+01	8.72E+00	4.64E+01
37.78	81.12	3.83E+01	8.93E+00	3.95E+01	8.59E+00	3.71E+01	8.17E+00	3.70E+01
44.88	63.52	3.26E+01	9.66E+00	3.31E+01	8.99E+00	3.22E+01	8.49E+00	3.56E+01
46.8	71.38	4.69E+01	1.82E+01	4.63E+01	1.76E+01	4.59E+01	1.74E+01	5.03E+01
43.9	69.93	4.07E+01	9.95E+00	4.01E+01	9.38E+00	4.04E+01	9.02E+00	4.21E+01

Mrange

X	Y	ESTIMATE	VARIANCE	ESTIMATE	VARIANCE	ESTIMATE	VARIANCE	Mrange
		Autokriging	121 points	Cokriging	121 points	Cokriging	121+56 points	Original
35.33	94.37	8.53E+01	3.12E+01	8.56E+01	3.09E+01	8.45E+01	2.50E+01	9.10E+01
34.73	92.23	8.37E+01	3.34E+01	8.39E+01	3.32E+01	8.25E+01	2.61E+01	8.70E+01
41.93	72.68	8.55E+01	2.51E+01	8.52E+01	2.49E+01	8.52E+01	2.15E+01	9.20E+01
38.85	77.03	8.38E+01	2.02E+01	8.31E+01	2.00E+01	8.09E+01	1.83E+01	8.40E+01
39.67	75.6	8.25E+01	2.05E+01	8.21E+01	2.04E+01	8.15E+01	1.86E+01	8.90E+01
30.22	81.88	7.61E+01	1.94E+01	7.51E+01	1.91E+01	7.51E+01	1.78E+01	7.90E+01
24.58	81.68	4.88E+01	2.21E+01	5.04E+01	2.15E+01	5.16E+01	1.99E+01	4.20E+01
32.52	84.95	8.45E+01	2.49E+01	8.46E+01	2.47E+01	8.46E+01	2.14E+01	8.50E+01
32.13	81.2	7.88E+01	2.30E+01	7.78E+01	2.27E+01	7.68E+01	2.02E+01	8.10E+01
41.98	87.9	8.83E+01	2.60E+01	8.84E+01	2.59E+01	8.83E+01	2.13E+01	9.20E+01
41.53	93.65	9.14E+01	2.97E+01	9.13E+01	2.95E+01	9.17E+01	2.42E+01	9.90E+01
42.08	87.83	8.80E+01	2.60E+01	8.81E+01	2.58E+01	8.80E+01	2.13E+01	9.10E+01
41.45	90.5	9.11E+01	2.82E+01	9.09E+01	2.80E+01	8.98E+01	2.33E+01	9.60E+01
40.67	89.68	9.17E+01	2.55E+01	9.13E+01	2.52E+01	9.08E+01	2.18E+01	9.60E+01
41	85.2	8.95E+01	2.45E+01	8.96E+01	2.44E+01	9.00E+01	2.12E+01	9.10E+01
38.03	84.6	9.59E+01	2.52E+01	9.51E+01	2.50E+01	9.48E+01	2.16E+01	9.70E+01
29.98	90.25	7.05E+01	2.12E+01	7.03E+01	2.09E+01	6.98E+01	1.91E+01	6.90E+01
38.28	76.42	8.30E+01	2.27E+01	8.22E+01	2.25E+01	8.12E+01	2.01E+01	8.10E+01
45.07	83.57	8.17E+01	3.26E+01	8.22E+01	3.23E+01	8.28E+01	2.60E+01	8.00E+01
42.97	83.75	8.35E+01	2.59E+01	8.38E+01	2.56E+01	8.47E+01	2.19E+01	9.00E+01
42.77	84.6	8.41E+01	2.46E+01	8.45E+01	2.44E+01	8.54E+01	2.11E+01	8.40E+01
46.83	92.18	9.23E+01	3.69E+01	9.26E+01	3.66E+01	9.43E+01	2.85E+01	8.60E+01
44.88	93.22	9.44E+01	3.13E+01	9.47E+01	3.10E+01	9.36E+01	2.53E+01	9.10E+01
38.82	92.22	9.01E+01	3.02E+01	9.02E+01	3.00E+01	9.12E+01	2.45E+01	9.30E+01
32.32	90.08	7.82E+01	2.89E+01	7.83E+01	2.87E+01	7.98E+01	2.37E+01	8.00E+01
32.33	88.75	7.95E+01	2.21E+01	7.99E+01	2.17E+01	8.05E+01	1.96E+01	8.30E+01
35.27	75.55	8.01E+01	3.44E+01	7.90E+01	3.41E+01	7.85E+01	2.68E+01	6.90E+01
35.22	80.93	8.71E+01	2.42E+01	8.78E+01	2.41E+01	8.80E+01	2.09E+01	8.30E+01
34.9	76.88	8.05E+01	2.50E+01	7.97E+01	2.47E+01	7.93E+01	2.14E+01	8.20E+01
46.9	96.8	9.94E+01	4.25E+01	9.88E+01	4.23E+01	9.51E+01	3.10E+01	8.80E+01
42.87	100.55	1.03E+02	3.22E+01	1.03E+02	3.20E+01	1.03E+02	2.56E+01	1.02E+02
39.45	74.57	8.34E+01	2.30E+01	8.28E+01	2.28E+01	8.26E+01	2.03E+01	8.80E+01
42.22	75.98	8.79E+01	2.28E+01	8.86E+01	2.26E+01	9.26E+01	2.01E+01	9.50E+01
40.65	73.78	8.13E+01	2.04E+01	8.08E+01	2.00E+01	7.95E+01	1.85E+01	7.10E+01
40.92	81.43	9.06E+01	2.26E+01	9.09E+01	2.24E+01	9.15E+01	2.00E+01	9.40E+01
35.4	97.6	8.87E+01	3.19E+01	8.87E+01	3.17E+01	8.92E+01	2.52E+01	8.40E+01
42.83	80.18	8.68E+01	2.57E+01	8.72E+01	2.55E+01	8.71E+01	2.20E+01	8.80E+01
40.5	80.22	8.99E+01	2.66E+01	9.01E+01	2.63E+01	9.20E+01	2.24E+01	9.30E+01
35.03	85.2	8.98E+01	2.79E+01	9.05E+01	2.77E+01	9.01E+01	2.30E+01	8.80E+01
35.8	84	9.22E+01	2.78E+01	9.31E+01	2.77E+01	9.26E+01	2.30E+01	1.01E+02
36.12	86.68	9.05E+01	2.89E+01	9.03E+01	2.87E+01	8.97E+01	2.37E+01	9.50E+01
32.42	99.68	8.97E+01	2.94E+01	9.04E+01	2.92E+01	9.17E+01	2.41E+01	8.90E+01
35.23	101.7	9.70E+01	3.42E+01	9.84E+01	3.39E+01	1.01E+02	2.68E+01	9.20E+01
25.9	97.43	7.49E+01	4.30E+01	7.41E+01	4.27E+01	7.18E+01	3.13E+01	7.40E+01
27.7	97.28	7.60E+01	2.04E+01	7.51E+01	2.02E+01	7.38E+01	1.87E+01	6.60E+01
32.9	97.03	8.77E+01	2.20E+01	8.69E+01	2.15E+01	8.64E+01	1.96E+01	8.40E+01
29.97	95.35	7.48E+01	2.79E+01	7.43E+01	2.77E+01	7.46E+01	2.33E+01	7.20E+01
29.53	98.47	8.19E+01	2.90E+01	8.18E+01	2.89E+01	8.40E+01	2.39E+01	8.90E+01
33.97	98.48	9.02E+01	3.31E+01	9.03E+01	3.29E+01	8.91E+01	2.58E+01	9.20E+01
36.93	76.28	8.19E+01	1.85E+01	8.10E+01	1.82E+01	8.10E+01	1.72E+01	7.90E+01
38.95	77.45	8.47E+01	2.17E+01	8.39E+01	2.15E+01	8.18E+01	1.93E+01	9.30E+01
42.95	87.9	8.60E+01	2.53E+01	8.63E+01	2.52E+01	8.60E+01	2.15E+01	8.60E+01
37.78	81.12	9.20E+01	2.35E+01	9.27E+01	2.33E+01	9.65E+01	2.06E+01	9.10E+01
44.88	63.52	6.85E+01	2.35E+01	6.90E+01	2.31E+01	7.11E+01	2.09E+01	6.80E+01
46.8	71.38	8.63E+01	4.52E+01	8.57E+01	4.50E+01	8.51E+01	3.20E+01	7.50E+01
43.9	69.93	8.62E+01	2.53E+01	8.51E+01	2.49E+01	8.37E+01	2.18E+01	9.10E+01

Temperature

X	Y	ESTIMATE	VARIANCE	ESTIMATE	VARIANCE	ESTIMATE	VARIANCE	TEMP
		Autokriging	121 points	Cokriging	121 points	Cokriging	121+56 points	Original
35.33	94.37	5.58E+01	1.76E+01	5.56E+01	1.74E+01	5.59E+01	1.72E+01	5.36E+01
34.73	92.23	6.01E+01	2.08E+01	5.98E+01	2.06E+01	6.00E+01	2.02E+01	5.72E+01
41.93	72.68	3.99E+01	1.06E+01	4.02E+01	1.04E+01	4.02E+01	1.04E+01	3.86E+01
38.85	77.03	4.63E+01	4.13E+00	4.70E+01	3.90E+00	4.62E+01	3.58E+00	4.67E+01
39.67	75.6	4.38E+01	5.36E+00	4.46E+01	5.07E+00	4.42E+01	4.86E+00	4.35E+01
30.22	81.88	6.80E+01	3.29E+00	6.83E+01	3.05E+00	6.83E+01	2.65E+00	6.83E+01
24.58	81.68	7.58E+01	1.96E+00	7.59E+01	1.58E+00	7.58E+01	9.13E-01	7.58E+01
32.52	84.95	6.14E+01	1.05E+01	6.12E+01	1.03E+01	6.13E+01	1.03E+01	6.17E+01
32.13	81.2	6.29E+01	7.38E+00	6.34E+01	7.09E+00	6.33E+01	7.00E+00	6.38E+01
41.98	87.9	3.51E+01	1.18E+01	3.52E+01	1.17E+01	3.53E+01	1.12E+01	3.58E+01
41.53	93.65	3.61E+01	1.62E+01	3.63E+01	1.60E+01	3.63E+01	1.59E+01	3.58E+01
42.08	87.83	3.50E+01	1.19E+01	3.51E+01	1.17E+01	3.52E+01	1.12E+01	3.66E+01
41.45	90.5	3.60E+01	1.45E+01	3.62E+01	1.44E+01	3.61E+01	1.43E+01	3.56E+01
40.67	89.68	3.74E+01	9.73E+00	3.76E+01	9.48E+00	3.76E+01	9.38E+00	3.68E+01
41	85.2	3.86E+01	1.04E+01	3.85E+01	1.02E+01	3.85E+01	1.02E+01	3.72E+01
38.03	84.6	4.99E+01	1.05E+01	4.99E+01	1.03E+01	5.01E+01	1.03E+01	5.19E+01
29.98	90.25	6.63E+01	3.93E+00	6.68E+01	3.64E+00	6.64E+01	3.28E+00	6.72E+01
38.28	76.42	4.97E+01	8.29E+00	5.03E+01	8.17E+00	4.99E+01	8.12E+00	4.87E+01
45.07	83.57	3.10E+01	1.86E+01	3.13E+01	1.85E+01	3.14E+01	1.82E+01	3.28E+01
42.97	83.75	3.45E+01	1.08E+01	3.48E+01	1.05E+01	3.48E+01	1.04E+01	3.45E+01
42.77	84.6	3.50E+01	9.59E+00	3.52E+01	9.37E+00	3.53E+01	9.28E+00	3.57E+01
46.83	92.18	2.57E+01	2.39E+01	2.57E+01	2.37E+01	2.53E+01	2.31E+01	2.48E+01
44.88	93.22	2.86E+01	1.65E+01	2.84E+01	1.62E+01	2.84E+01	1.61E+01	3.00E+01
38.82	92.22	4.46E+01	1.68E+01	4.44E+01	1.66E+01	4.42E+01	1.64E+01	4.30E+01
32.32	90.08	6.45E+01	1.54E+01	6.43E+01	1.53E+01	6.40E+01	1.52E+01	6.30E+01
32.33	88.75	6.27E+01	4.50E+00	6.23E+01	4.12E+00	6.25E+01	3.80E+00	6.34E+01
35.27	75.55	5.93E+01	2.16E+01	5.98E+01	2.13E+01	5.98E+01	2.08E+01	5.88E+01
35.22	80.93	5.57E+01	9.99E+00	5.52E+01	9.82E+00	5.54E+01	9.81E+00	5.58E+01
34.9	76.88	6.01E+01	8.62E+00	6.04E+01	8.27E+00	6.04E+01	8.10E+00	6.16E+01
46.9	96.8	2.69E+01	3.29E+01	2.72E+01	3.28E+01	2.89E+01	3.10E+01	2.57E+01
42.87	100.55	3.68E+01	1.95E+01	3.66E+01	1.93E+01	3.63E+01	1.90E+01	3.83E+01
39.45	74.57	4.72E+01	7.57E+00	4.79E+01	7.27E+00	4.79E+01	7.18E+00	4.62E+01
42.22	75.98	3.74E+01	7.63E+00	3.68E+01	7.43E+00	3.76E+01	7.36E+00	3.52E+01
40.65	73.78	4.41E+01	3.03E+00	4.50E+01	2.64E+00	4.44E+01	2.20E+00	4.30E+01
40.92	81.43	4.07E+01	6.82E+00	4.04E+01	6.63E+00	4.08E+01	6.50E+00	4.06E+01
35.4	97.6	5.34E+01	1.90E+01	5.36E+01	1.89E+01	5.35E+01	1.84E+01	5.29E+01
42.83	80.18	3.59E+01	1.07E+01	3.57E+01	1.05E+01	3.60E+01	1.05E+01	3.92E+01
40.5	80.22	4.17E+01	1.15E+01	4.12E+01	1.12E+01	4.10E+01	1.12E+01	4.14E+01
35.03	85.2	5.36E+01	1.44E+01	5.29E+01	1.42E+01	5.30E+01	1.40E+01	5.51E+01
35.8	84	5.21E+01	1.49E+01	5.11E+01	1.47E+01	5.15E+01	1.46E+01	5.30E+01
36.12	86.68	5.15E+01	1.49E+01	5.16E+01	1.47E+01	5.17E+01	1.46E+01	5.53E+01
32.42	99.68	6.03E+01	1.57E+01	5.97E+01	1.55E+01	5.97E+01	1.53E+01	6.06E+01
35.23	101.7	5.28E+01	2.01E+01	5.19E+01	1.99E+01	5.13E+01	1.96E+01	5.22E+01
25.9	97.43	7.18E+01	3.21E+01	7.27E+01	3.16E+01	7.33E+01	3.01E+01	7.25E+01
27.7	97.28	7.00E+01	3.96E+00	7.06E+01	3.63E+00	7.01E+01	3.23E+00	6.80E+01
32.9	97.03	6.09E+01	3.38E+00	6.11E+01	2.94E+00	6.10E+01	2.48E+00	6.05E+01
29.97	95.35	6.66E+01	1.36E+01	6.70E+01	1.34E+01	6.70E+01	1.34E+01	6.80E+01
29.53	98.47	6.68E+01	1.57E+01	6.66E+01	1.54E+01	6.61E+01	1.53E+01	6.60E+01
33.97	98.48	5.71E+01	2.12E+01	5.69E+01	2.10E+01	5.68E+01	2.03E+01	5.72E+01
36.93	76.28	5.59E+01	1.97E+00	5.63E+01	1.57E+00	5.59E+01	9.94E-01	5.61E+01
38.95	77.45	4.57E+01	5.88E+00	4.65E+01	5.64E+00	4.58E+01	5.45E+00	4.39E+01
42.95	87.9	3.37E+01	1.13E+01	3.39E+01	1.12E+01	3.39E+01	1.10E+01	3.46E+01
37.78	81.12	5.07E+01	8.03E+00	5.01E+01	7.82E+00	5.10E+01	7.75E+00	4.60E+01
44.88	63.52	3.66E+01	4.38E+00	3.65E+01	4.01E+00	3.72E+01	3.63E+00	3.58E+01
46.8	71.38	3.18E+01	3.74E+01	3.21E+01	3.72E+01	3.25E+01	3.47E+01	2.80E+01
43.9	69.93	3.63E+01	7.49E+00	3.70E+01	7.07E+00	3.68E+01	6.94E+00	3.54E+01